Lithos 300–301 (2018) 261–277

Contents lists available at ScienceDirect

Lithos

journal homepage: www.elsevier.com/locate/lithos

Relict zircon U-Pb age and O isotope evidence for reworking of Neoproterozoic crustal rocks in the origin of Triassic S-type granites in South China

Peng Gao [a,*], Yong-Fei Zheng [a], Yi-Xiang Chen [a], Zi-Fu Zhao [a], Xiao-Ping Xia [b]

[a] CAS Key Laboratory of Crust-Mantle Materials and Environments, School of Earth and Space Sciences, University of Science and Technology of China, Hefei 230026, China
[b] State Key Laboratory of Isotope Geochemistry, Guangzhou Institute of Geochemistry, Chinese Academy of Sciences, Guangzhou 510640, China

ARTICLE INFO

Article history:
Received 11 June 2017
Accepted 25 November 2017
Available online 5 December 2017

Keywords:
Granites
Relict zircon
Magmatic zircon
Peritectic zircon
Transient melting

ABSTRACT

Granites derived from partial melting of sedimentary rocks are generally characterized by high $\delta^{18}O$ values and abundant relict zircons. Such relict zircons are valuable in tracing the source rocks of granites and the history of crustal anatexis. Here we report in-situ U-Pb ages, O isotopes and trace elements in zircons from Triassic granites in the Zhuguangshan and Jiuzhou regions, which are located in the Nanling Range and the Darongshan area, respectively, in South China. Zircon U-Pb dating yields magma crystallization ages of 236 ± 2 Ma for the Zhuguangshan granites and 246 ± 2 Ma to 252 ± 3 Ma for the Jiuzhou granites. The Triassic *syn*-magmatic zircons are characterized by high $\delta^{18}O$ values of 10.1–11.9‰ in Zhuguangshan and 8.5–13.5‰ in Jiuzhou. The relict zircons show a wide range of U-Pb ages from 315 to 2185 Ma in Zhuguangshan and from 304 to 3121 Ma in Jiuzhou. Nevertheless, a dominant age peak of 700–1000 Ma is prominent in both occurrences, demonstrating that their source rocks were dominated by detrital sediments weathered from Neoproterozoic magmatic rocks. Taking previous results for regional granites together, Neoproterozoic relict zircons show $\delta^{18}O$ values in a small range from 5 to 8‰ for the Nanling granites but a large range from 5 to 11‰ for the Darongshan granites. In addition, relict zircons of Paleozoic U-Pb age occur in the two granitic plutons. They exhibit consistently high $\delta^{18}O$ values similar to the Triassic *syn*-magmatic zircons in the host granites. These Paleozoic relict zircons are interpreted as the peritectic product during transient melting of the metasedimentary rocks in response to the intracontinental orogenesis in South China. Therefore, the relict zircons of Neoproterozoic age are directly inherited from the source rocks of S-type granites, and those of Paleozoic age record the transient melting of metasedimentary rocks before intensive melting for granitic magmatism in the Triassic.

1. Introduction

Granites are produced primarily by partial melting of crustal rocks and they are widespread in continental regions (Brown, 2013). Deciphering the origin of granites has great bearing on understanding continental differentiation and their genetic link to contemporaneous mineralization (e.g., Brown, 2013; Kemp et al., 2007; Kemp and Hawkesworth, 2003). Relict zircon is common in granites sourced from sedimentary rocks. It has been employed to unravel the preservation of source heterogeneity in granites (Villaros et al., 2012), to recover the history of crustal reworking (Jeon et al., 2014), and to distinguish sedimentary rocks-derived granites from highly fractionated igneous rock-derived granites (Gao et al., 2016a). In doing so, the origin of relict zircon must be clarified at first because a granite may be derived from partial melting of various source rocks, which were mingled either before anatexis (source mixing) or after anatexis (magma mixing). Although xenocryst zircon could occur in granites due to wallrock contamination (e.g., Miller et al., 2007), its source would be adjacent to the emplacement site of granites. In this regard, the xenocryst zircon may be present in small xenoliths which were not completely digested by granitic magmas. As a consequence, the xenoliths often show distinct mineral paragenesis from host granites. Therefore, relict zircon in granites is primarily inherited from their source rocks, providing a powerful means to trace the nature of crustal sources. However, there are different origins of relict zircon in granites (Chen and Zheng, 2017), which have not been well discriminated in previous studies. This seriously limits our understanding of granite petrogenesis with respect to its source nature.

Triassic granites in South China are mostly peraluminous and produced by reworking of crustal rocks (e.g., Gao et al., 2017; Wang et al., 2013; Zhou et al., 2006). Based on the temporal-spatial distributions of these granites as well as structural, sedimentary and metamorphic records, various models have been proposed for their petrogenesis,

* Corresponding author.
E-mail address: gaopeng05@ustc.edu.cn (P. Gao).

https://doi.org/10.1016/j.lithos.2017.11.036
0024-4937/

including flat-subduction of the Pacific slab (Li and Li, 2007) and intracontinental reworking (Gao et al., 2017; Wang et al., 2013). Because of their sporadic outcrop in a broad (~1300 km width) intracontinental region, the relationship between their petrogenesis and collisional orogeny has been controversial. Previous understanding of the source nature of Triassic granites mainly relies on whole-rock Nd and zircon Hf isotope compositions. Extensive investigations have determined that these Triassic granites have a range of whole-rock $\varepsilon_{Nd}(t)$ values from −11.3 to −6.4 and two-stage Nd model ages of 1.7–2.0 Ga (e.g., Chen and Jahn, 1998; Deng et al., 2004; Gao et al., 2014; Hsieh et al., 2008; Wang et al., 2007a; Zhao et al., 2013, 2015), suggesting their derivation from reworking of ancient Paleoproterozoic crust. However, zircon $\varepsilon_{Hf}(t)$ values and Hf model ages are more varied, ranging from −29.0 to −1.8 and from 1.2 to 3.3 Ga, respectively (e.g., Chen et al., 2012; Gao et al., 2014; Jiao et al., 2015; Qi et al., 2007; Song et al., 2016; Zhao et al., 2013), suggesting involvement of ancient Mesoproterozoic to Archean crust. Although these whole-rock Nd and zircon Hf model ages are used to indicate the age of crustal sources, it does not mean that the source crust has such formation ages. Instead, the formation age of granite sources can be directly dated by relict zircons in granites.

In this paper, we present a combined study of U-Pb ages, O isotopes and trace elements for zircons from Triassic granites in two locations. One is the southern Zhuguangshan complex, which is adjacent to the Guidong complex (Fig. 1a). Both complexes are located in the Nanling Range (Fig. 1a). Therefore, data from the southern Zhuguangshan complex provide a supplement to previous observations from the Nanling Range. The other is the Darongshan batholith, from which more samples were selected because systematic data on U-Pb ages, O isotopes and trace elements were absent. In combination with previous data and our petrological investigations, we are in position to discriminate different origins of relict zircons. The results not only place a geochronological constraint on the source rocks of Triassic granites but also provide a geochemical insight into the history of crustal anatexis during the Paleozoic in South China.

2. Geological setting and samples

The present study deals with Triassic granites in the Nanling Range and the Darongshan batholith in South China (Fig. 1a). Tectonically, South China is composed of three petrotectonic units, the Yangtze craton in the northwest, the Cathaysian terrane in the southeast, and the Jiangnan orogen in between (e.g., Zhao, 2015; Zheng et al., 2013). The Nanling Range is located in the western Cathaysian terrane whereas the Darongshan batholith is located in the southern part of the Jiangnan orogen. The Jiangnan orogen was built by subduction of the Cathaysian oceanic slab beneath the Yangtze craton in the Late Mesoproterozoic to Early Neoproterozoic (Zhang and Zheng, 2013), with the extensive generation of arc magmatic rocks (Fig. 1a). Afterwards South China underwent multiple episodes of intracontinental reworking, resulting in the formation of bimodal magmatic rocks mainly at 830 to 750 Ma in the Middle Neoproterozoic and voluminous migmatites and granites mainly at 450–420 Ma in the Early Paleozoic (Z.X. Li et al., 2010; Wang et al., 2013; Zhang and Zheng, 2013). In the Triassic, South China collided with North China in the north and with Indochina in the south (Zheng et al., 2013), leading to establishment of the bulk tectonic framework for eastern China (e.g., Huang et al., 1987). Intensive tectonism was developed in this period, including stratigraphic unconformities, metamorphism and orogenic magmatism (Gao et al., 2017; Wang et al., 2013; Zhou et al., 2006). The Triassic magmatic rocks are predominantly granites, which are mostly located in the region between the Zhenghe-Dapu Fault and the Anhua-Luocheng Fault. This region is largely overlapped on the Neoproterozoic rocks in the western Cathaysian terrane and the Jiangnan orogen (Fig. 1a).

Samples used in this study are granites from the southern Zhuguangshan complex in the Nanling Range (Fig. 1b) and the Jiuzhou pluton in the Darongshan batholith (Fig. 1c). The southern Zhuguangshan complex, located in the northern Guangdong province with a outcrop area of ca. 1500 km^2, is composed of dominant Triassic granites and minor Paleozoic granites and migmatites in the east, and numerous Jurassic-Cretaceous granites in the west (Deng et al., 2012). The Triassic rocks mainly consist of biotite granites. The Darongshan batholith crops out in an area of >10,000 km^2 in a NE-SW strike with only the Triassic age (Chen et al., 2011; Jiao et al., 2015; Zhao et al., 2012). From north to south, it is mainly composed of the Darongshan, Pubei, Taima and Jiuzhou plutons (Fig. 1c). The Darongshan and Pubei plutons consist mainly of cordierite-biotite granites, whereas the Taima pluton is mainly composed of orthopyroxene-bearing granite porphyry. The major rock type in the Jiuzhou pluton is hypersthene-cordierite-biotite granite. These four

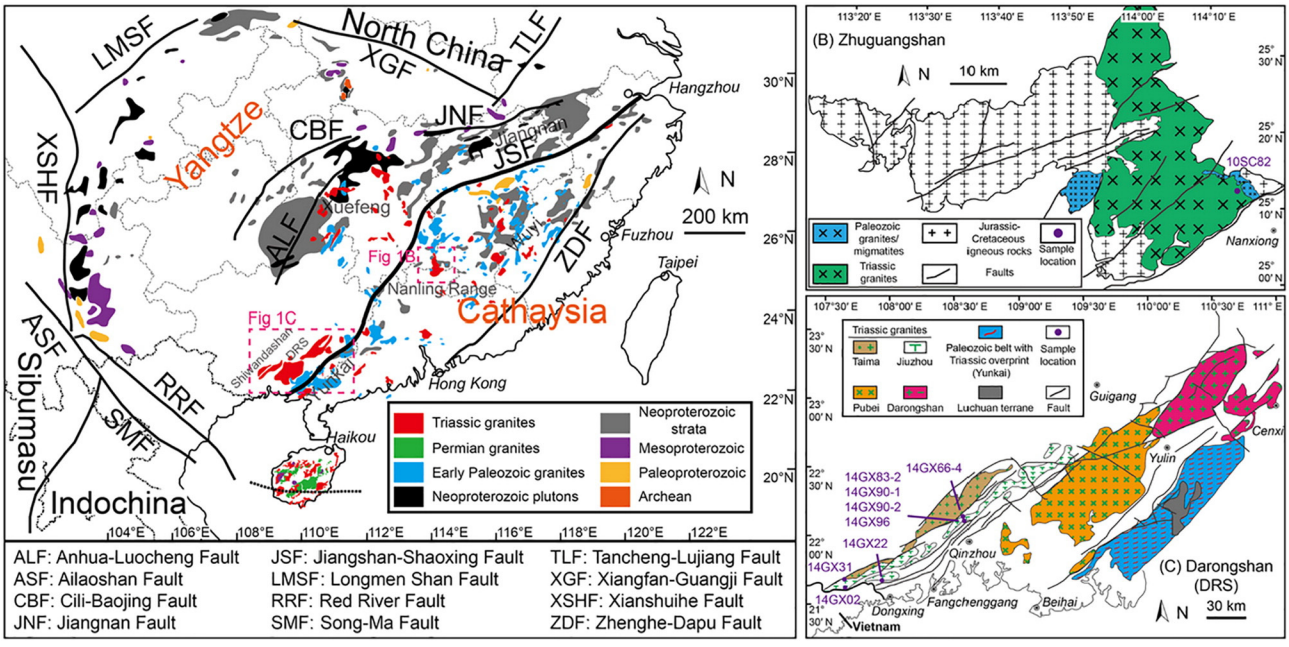

Fig. 1. A: Distributions of magmatic rocks in South China (modified after Wang et al., 2013, and Zhang and Zheng, 2013). Schematic geological maps of the southern Zhuguangshan granitic complex (B; modified after Deng et al., 2012) and the Darongshan batholith (C; modified after Zhao et al., 2012 and Jiao et al., 2015), showing sample sites.

plutons were suggested to share common metasedimentary sources, but be produced by partial melting under different pressure-temperature (P-T) conditions (Jiao et al., 2015; Zhao et al., 2017a).

We have selected one sample from the southern Zhuguangshan granite and eight samples from the Jiuzhou granite for the present study. The southern Zhuguangshan biotite granites are gray to dark gray in color, medium- to coarse-grained with massive structure. Some granites show porphyritic texture with phenocryst of K-feldspar. They are primarily composed of quartz, K-feldspar, plagioclase and minor biotite with accessory minerals of zircon, apatite, monazite, and ilmenite. The Jiuzhou granites are generally dark gray in color and show massive structure. They are mainly composed of quartz, plagioclase, K-feldspar, biotite, orthopyroxene, cordierite, and garnet. Most phenocrysts are K-feldspar. Biotite, orthopyroxene and garnet occur occasionally as phenocrysts. Accessory minerals include apatite, monazite, zircon, and ilmenite, with occasional presence of tourmaline and secondary muscovite and chlorite.

The Jiuzhou pluton in the Darongshan batholith was selected for the following three reasons: (1) Qiao et al. (2015) studied only one sample from this pluton but four from the Taima pluton and three from the Pubei pluton; (2) this pluton contains abundant granulite enclaves, which were suggested to be the restite after extraction of granitic melts (e.g., Jiao et al., 2013; Zhao et al., 2012, 2017b); (3) the Jiuzhou granites were termed as charnockite by Jiao et al. (2015). Our further work will focus on a petrological and mineralogical comparison between the enclaves and their host granite.

3. Analytical methods

Zircon grains were extracted, mounted and polished to expose the grain center for microbeam analysis. Cathodoluminescence (CL) images are taken for inspecting internal structures of individual zircons and selecting positions for in-situ analyses. CL images for representative relict zircon grains are shown in Figs. 2 and 3.

3.1. SIMS in-situ zircon U-Pb dating

The U-Pb isotopic compositions of some zircon cores with small sizes were measured on a Cameca IMS 1280-HR at State Key Laboratory of Isotope Geochemistry in Guangzhou Institute of Geochemistry, Chinese Academy of Sciences (CAS), Guangzhou. Operating and data processing procedures are similar to those described by Li et al. (2009). Analyses of unknown samples were interspersed with standards. Sample U-Th-Pb isotope ratios were calibrated relative to the standard zircon Plěsovice which has a $^{206}Pb/^{238}U$ ratio of 0.05369, corresponding to an age of 337.1 Ma (Sláma et al., 2008), and the absolute abundances of U, Th and Pb were determined relative to the standard zircon M257 that has U = 840 ppm and Th/U = 0.27 (Nasdala et al., 2008). A long-term uncertainty of ±1.5% (1 RSD) has been found for $^{206}Pb/^{238}U$ measurements of the standard zircons (Q.L. Li et al., 2010), which was propagated to the unknowns. The measured $^{206}Pb/^{238}U$ errors during the course of this study are about ±1% (1 RSD) before considering the external error.

The ^{204}Pb-method was used for correcting the common Pb in measured Pb isotopic compositions. Due to the extremely small corrections, an average present-day crustal composition is used for the common Pb (Stacey and Kramers, 1975), assuming that the common Pb is largely surface contamination introduced during sample preparation. Uncertainties in individual analyses are reported at a 1σ level in data tables. Mean ages for pooled U/Pb analyses are quoted with 95% confidence interval. Data processing was carried out with the Isoplot/Ex 3 software (Ludwig, 2003). A secondary standard zircon Qinghu was analyzed as an unknown to monitor the reliability of the whole procedure. Twenty concordant analyses of Qinghu during the course of this study yield a mean $^{206}Pb/^{238}U$ age of 159.1 ± 1.1 Ma (MSWD = 1.0), consistent within errors with its recommended value of 159.5 ± 0.2 Ma (Li et al., 2013). All U-Pb isotope data are listed in Supplementary Table S1. Zircon U-Pb ages with discordance larger than ±10% were discarded in geological interpretation.

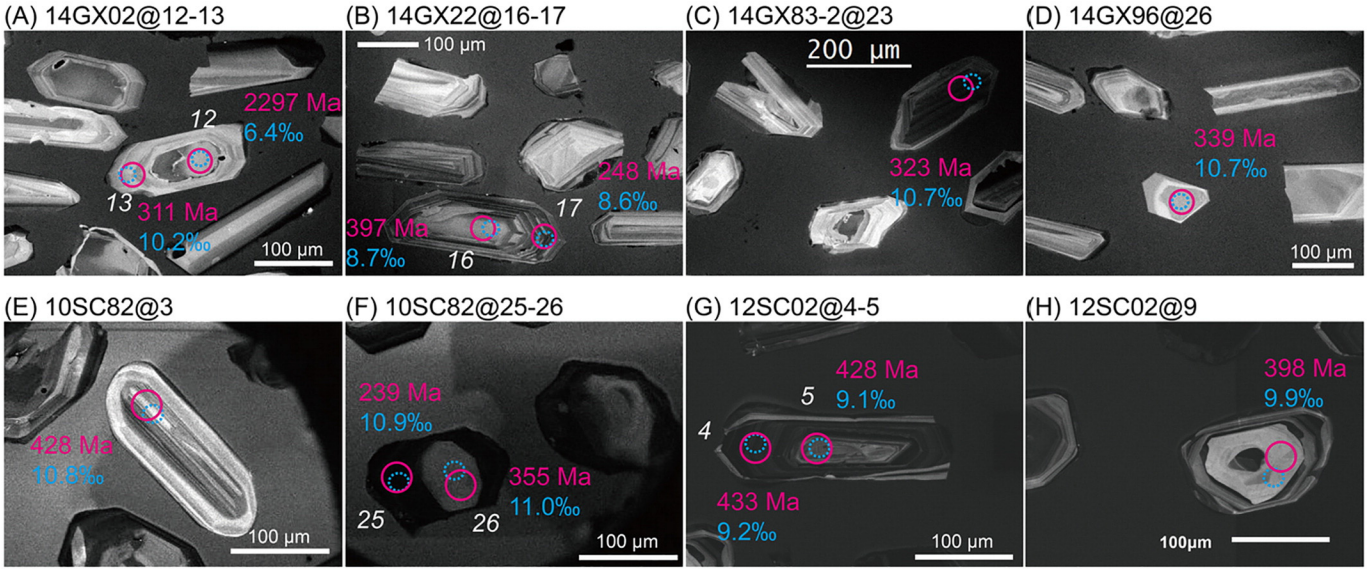

Fig. 2. CL images of representative peritectic zircons from Triassic granites in the Jiuzhou pluton (A–D), the southern Zhuguangshan complex (E–F) and the Xiazhuang pluton (G-H). The latter two granites are from the Nanling Range. The rose red circles and blue ellipses are analytical positions of U-Pb and O isotopes, with diameters of 32 μm and ca. 20 μm. Analytical results of U-Pb ages and $\delta^{18}O$ values are also labeled. The white italic numbers denote the analytical numbers. The data of the Xiazhuang pluton is taken from Gao et al. (2016a). Peritectic zircons occur as cores overgrown by Triassic rims or as separate grains without overgrowth rims. Peritectic zircons show unzoning to oscillatory zoning, but they generally have rounding rims, indicating dissolution into melts. Particularly, peritectic zircons have similarly high $\delta^{18}O$ values as the Triassic zircons grains.

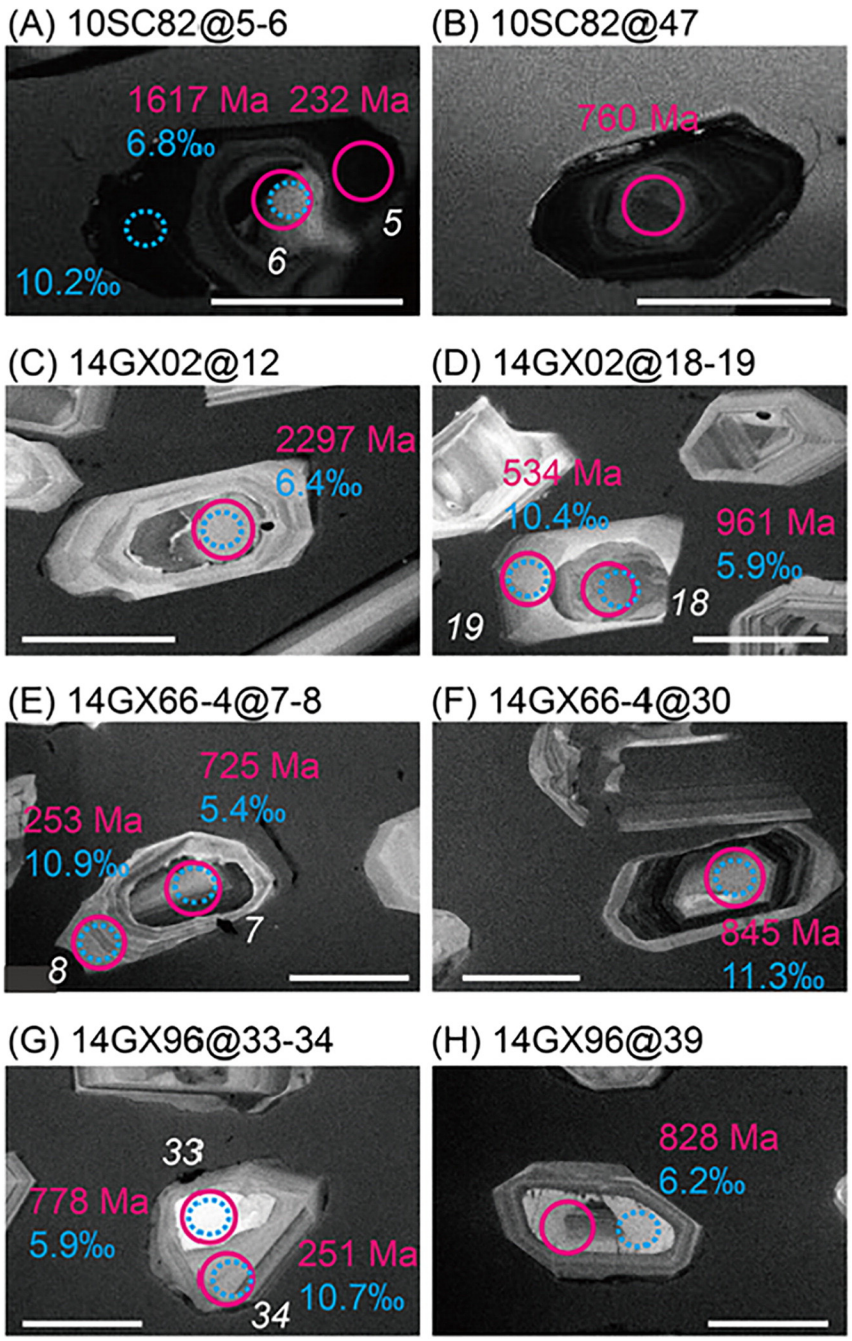

Fig. 3. CL images of representative relict zircons with detrital origin from Triassic granites in the southern Zhuguangshan complex (A–B) and the Jiuzhou pluton (C–H). The rose red circles and blue ellipses are analytical positions of U-Pb and O isotopes, with diameters of 32 μm and ca. 20 μm. Analytical results of U-Pb ages and $\delta^{18}O$ values are also labeled. The white italic numbers denote the analytical numbers.

3.2. SIMS in-situ zircon O isotope analysis

Zircon in-situ O isotopes were analyzed using Cameca IMS 1280-HR at State Key Laboratory of Isotope Geochemistry in Guangzhou Institute of Geochemistry, CAS, Guangzhou. Analytical procedures are the same as those described by Li et al., 2010a. The Cs^+ primary ion beam was accelerated at 10 kV, with an intensity of ca. 2 nA (Gaussian mode with a primary beam aperture of 200 μm to reduce aberrations) and rastered over a 10 μm area. The analysis spot was about 20 μm in diameter (10 μm beam diameter + 10 μm raster). Oxygen isotopes were measured in multi-collector mode using two off-axis Faraday cups. The NMR (Nuclear Magnetic Resonance) probe was used for magnetic field control with stability better than 2.5 ppm over 16 h on mass 17. One analysis takes ~3.5 min consisting of pre-sputtering (~30 s), 120 s of automatic tuning of the secondary beam, and 64 s of analysis. The instrumental mass fractionation (IMF) was corrected using in-house zircon standard Penglai with a recommended $\delta^{18}O$ value of 5.31 ± 0.10‰ with reference to the Vienna standard mean oceanic water (VSMOW) that has a recommended $^{18}O/^{16}O$ ratio of 0.0020052 (Li et al., 2010b). The measured $^{18}O/^{16}O$ ratios for samples (raw data) were firstly normalized relative to the VSMOW, and then corrected for IMF (Li et al., 2010a).

The internal precision of a single analysis was generally better than ±0.20‰ (2σ standard error) for $\delta^{18}O$ values. The external precision, measured by the reproducibility of repeated analyses of the Penglai

standard during three sessions of this study, is ±0.41‰ (2SD, n = 38), ±0.34‰ (2SD, n = 34) and ±0.34‰ (2SD, n = 50). During the three sessions, a second zircon standard Qinghu was measured as an unknown to ascertain the veracity of the IMF. Three series of analyses in twenty, eighteen and twenty-six measurements, respectively, of Qinghu zircon standard yield a weighted mean of $\delta^{18}O$ = 5.51 ± 0.30‰ (2SD), 5.51 ± 0.36‰ (2SD) and 5.53 ± 0.53‰ (2SD). These values are in good agreement within errors with a reported value of 5.4 ± 0.2‰ (Li et al., 2013). Zircon O isotope data are listed in Supplementary Table S1.

3.3. LA-ICPMS zircon U-Pb isotope and trace element analyses

Zircon U–Pb isotope and trace element analyses were carried out using LA-ICPMS at School of Resources and Environmental Engineering in Hefei University of Technology, Hefei. A pulsed 193 nm ArF Excimer (COMPex PRO) with laser power of 10 mJ/cm^2 pulse energy at a repetition ratio of 6 Hz coupled to an Agilent 7500a quadrupole ICP-MS was used for ablation. Helium was used as carrier gas to provide efficient aerosol transport to the ICP and minimize aerosol deposition. The diameter of the laser ablation crater was 32 μm. Zircon 91,500 was used as an external standard to normalize isotopic fractionation during isotope analysis. NIST610 glass was used as an external standard to normalize U, Th and Pb concentrations of the unknowns. Meanwhile, zircon standard Plešovice was used for monitoring of the data quality. The detailed analytical procedure can be found in Liu et al. (2010). Mean ages for pooled U/Pb analyses are quoted with 95% confidence interval. Sixty-nine analyses of Plěsovice yield a mean $^{206}Pb/^{238}U$ age of 336.6 ± 1.8 Ma (MSWD = 0.3), consistent within errors with the ID-TIMS result of 337.13 ± 0.37 Ma (2σ) (Sláma et al., 2008).

The zircon trace element analysis was simultaneously obtained during the zircon U–Pb dating. NIST610 was used as an external standard to calculate the trace element contents of the unknowns, and the preferred values of element concentrations for the USGS reference glasses are from the GeoReM database (http://georem.mpch-mainz.gwdg.de/). The average analytical error ranges from ±10% for light rare earth elements (LREE) to ±5% for other trace elements. Off-line selection and integration of background and analyte signals, time-drift correction and quantitative calibration for U-Th-Pb dating were performed by ICPMSDataCal (Liu et al., 2010), and the common Pb correction was carried out using the EXCEL program of ComPbCorr#151 (Andersen, 2002).

3.4. Identification of crystal inclusions in zircon

Crystal inclusions in zircon were identified by the JY Horiba LabRam HR Evolution microprobe with a 532 nm Ar laser excitation at CAS Key Laboratory of Crust-Mantle Materials and Environments at University of Science and Technology of China, Hefei. The beam size for Raman spectroscopy was set at ~1 μm. Monocrystalline silicon and polystyrene were analyzed during the analytical session to monitor the precision and accuracy of the Raman data.

4. Results

The zircon U-Pb isotopic data are listed in Supplementary Table S1 and trace element data are listed in Supplementary Table S2. For zircon with U-Pb ages older than 1.0 Ga, $^{207}Pb/^{206}Pb$ ages are used in discussion; otherwise $^{206}Pb/^{238}U$ ages are used. The trace element data that are affected by the presence of crystal inclusions are precluded from the dataset.

4.1. Zircon U-Pb ages

Zircon U-Pb isotopic analyses were carried out on a total of nine samples and the results are plotted in concordia diagrams (Fig. 4), in which concordant (discordance ≦ ±10%) and discordant analyses (discordance > ±10%) are labeled separately.

Zircons from the Zhuguangshan sample are generally euhedral and mostly 100–300 μm in length with length/width ratios of ~1:1 to 3:1. Oscillatory zoning is common in CL images, and some relict zircon cores can be recognized with generally higher CL brightness (Figs. 2 and 3). Twenty-six concordant U-Pb ages were obtained on zircons with oscillatory zoning, giving a weighted mean $^{206}Pb/^{238}U$ age of 236 ± 2 Ma (MSWD = 2.2; Table S1). Abundances of U and Th vary from 159 ppm to 1045 ppm and from 89.6 ppm to 279 ppm, respectively, with Th/U ratios of 0.13–0.83 (Table S2). Seventeen analyses on relict cores yield concordant U-Pb ages varying from 315 ± 5 Ma to 2185 ± 64 Ma. They have relatively low contents of U (69.8–630 ppm) and Th (31.9–266 ppm) and variable Th/U ratios of 0.09–0.83 (Table S2).

As shown in representative CL images (Figs. 2 and 3), zircon grains from the eight Jiuzhou samples exhibit similar morphologies. They are generally euhedral and mostly 200–300 μm in length with length/width ratios of ~1.5:1 to 4:1. Most of them are characterized by oscillatory zoning. A subset of them contains relict cores. Ten to twenty-six concordant U-Pb ages were obtained on zircons with oscillatory zoning, yielding weighted mean $^{206}Pb/^{238}U$ ages of 246 ± 2 (MSWD = 1.2) to 252 ± 3 Ma (MSWD = 0.5; Table S1). There are no differences in Th and U concentrations as well as Th/U ratios for these zircons, with the majority of them falling in the range of 40–200 ppm, 140–650 ppm and 0.15–0.57, respectively (Table S2). Two to twenty concordant U-Pb ages were obtained on relict cores from the eight samples. A total of 57 analyses yield a large range of ages from 304 ± 16 Ma to 3121 ± 30 Ma, with the majority of them in the interval of 400–1100 Ma and a dominant peak at 700–1000 Ma (Fig. 5). Most of the relict zircons have U and Th concentrations lower than 1000 ppm and 400 ppm, respectively, and Th/U ratios in a range of 0.20–1.0 (Table S2).

In summary, the present U-Pb dating yields concordant Triassic ages of 236 ± 2 Ma for zircon from the Zhuguangshan granites and 246 ± 2 Ma to 252 ± 3 Ma for zircon from the Jiuzhou granites. Such Triassic ages are consistent with previous dates for the crystallization age of granitic magmas (Jiao et al., 2015; Qiao et al., 2015) and thus these target zircons are of *syn*-magmatic origin. On the other hand, there are many zircons showing variable pre-Triassic U-Pb ages from 315 to 2185 Ma in Zhuguangshan and from 304 to 3121 Ma in Jiuzhou. These old zircons ages are clearly of relict origin.

4.2. Zircon O isotopes

The zircons of Triassic U-Pb ages from the Zhuguangshan sample show high $\delta^{18}O$ values of 10.1–11.9‰ (Fig. 6a). For the Jiuzhou samples, the zircons of Triassic U-Pb ages from sample 14GX22 exhibit lower $\delta^{18}O$ values of 8.5–9.5‰ whereas those from sample 10SC31 show higher $\delta^{18}O$ values of 9.2–13.0‰ (most in the range of 9.2–10.2‰), and those from the other six samples exhibit consistently higher values of 10.0–13.5‰ (Fig. 6a). In contrast, relict zircons with pre-Triassic U-Pb ages show more variable $\delta^{18}O$ values from 5.1 to 11.6‰ for the Zhuguangshan sample and from 5.1 to 12.7‰ for the Jiuzhou samples.

4.3. Zircon trace elements and crystal inclusions

As shown in Fig. 6, Ti concentrations and Th/U ratio decrease but Yb/Gd ratio increases with increasing Hf concentrations in the zircon of Triassic U-Pb ages, suggesting that zircon growth is associated with the evolution of granitic magmas (Claiborne et al., 2010). The decrease of Ti with magma evolution as monitored by the Hf increase indicates a drop in magma temperatures and thus crystallization of Ti-rich phases such as biotite and ilmenite. The decrease of Th/U ratios with increasing Hf may be caused by growth of Th-rich minerals such as monazite. Similarly, the increase of Yb/Gd ratios with magma evolution suggests the progressive depletion of middle REE relative to heavy REE in granitic

melts as zircon crystallization proceeds, probably due to the growth of apatite and monazite.

The Triassic zircons from the Nanling granites show a large range of Th/U ratios from 0.06 to 2.6, whereas those from the Darongshan granites exhibit a limited range of Th/U ratios from 0.03 to 1.0 (Fig. 6c). On the other hand, pre-Triassic zircons show highly variable Th/U ratios of 0.09–2.1 for the Nanling granites and 0.03–3.2 for the Darongshan granites. Crystal inclusions are present in the zircons of Paleozoic U-Pb ages (Fig. 7). They are tiny mineral assemblages composed of muscovite, albite, quartz and K-feldspar.

5. The source rocks of Triassic granites

5.1. Previous understanding and its deficiency

Granites are a dominant constitute of the continental crust. Their origin is closely related to reworking of ancient and juvenile crustal rocks (e.g., Brown, 2013; Kemp et al., 2007). The source rocks of granites can be inferred from the petrological, mineralogical and geochemical characteristics of granites. Through characterizing the U-Pb age pattern of relict zircons in granites and the O isotope compositions of *syn*-magmatic zircons, it is known that Triassic granites in the Nanling

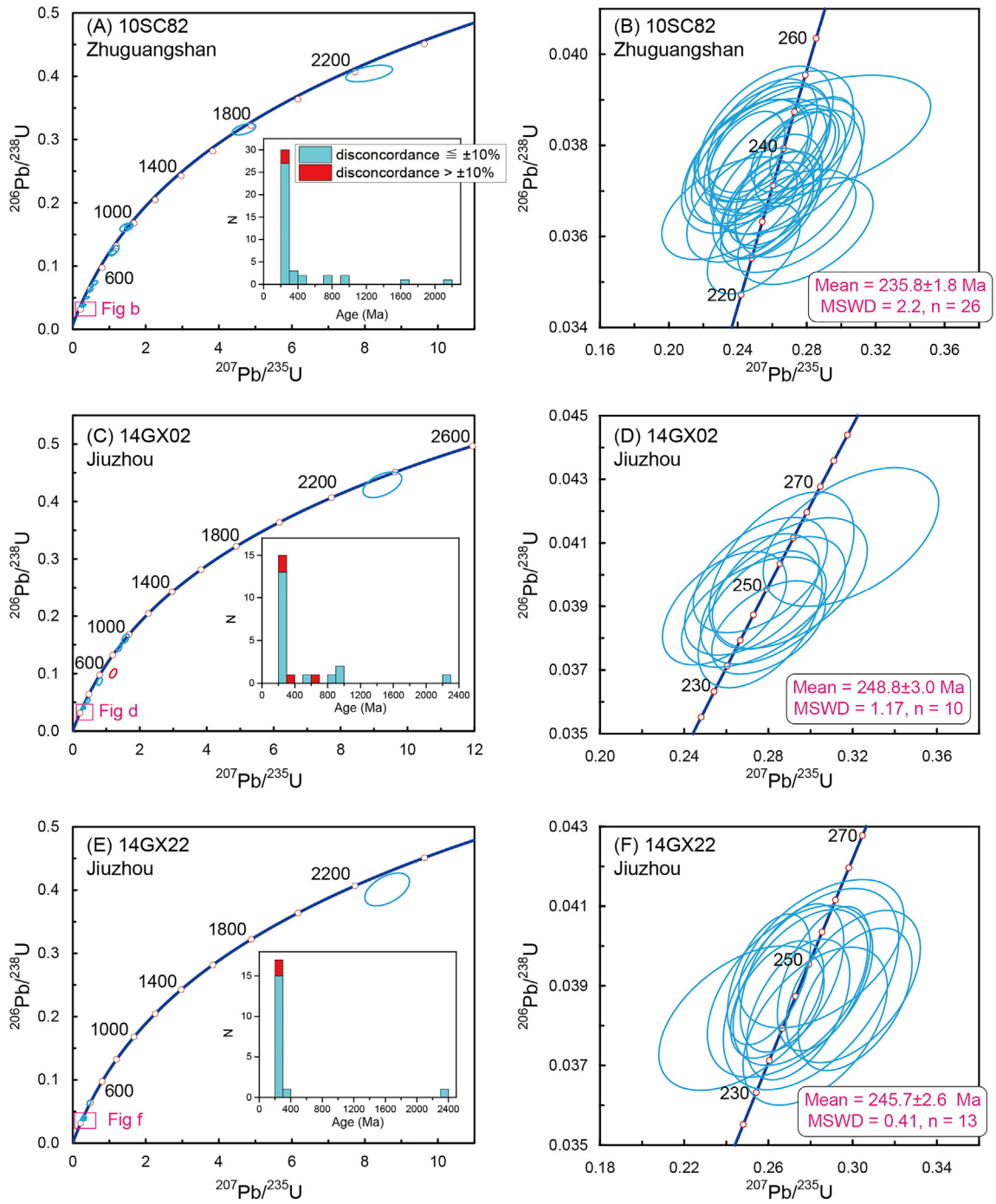

Fig. 4. Zircon U-Pb concordia diagrams for Triassic granites from the southern Zhuguangshan complex and the Jiuzhou pluton in South China. Left panels: the concordia diagrams for all analytical results grouped by concordance and the inserted plots showing the histograms; right panels: the concordia diagrams for Triassic *syn*-magmatic zircons showing the weighted mean ages of concordant analyses (discordance ≤10%). Note all data-point error ellipses are 2σ.

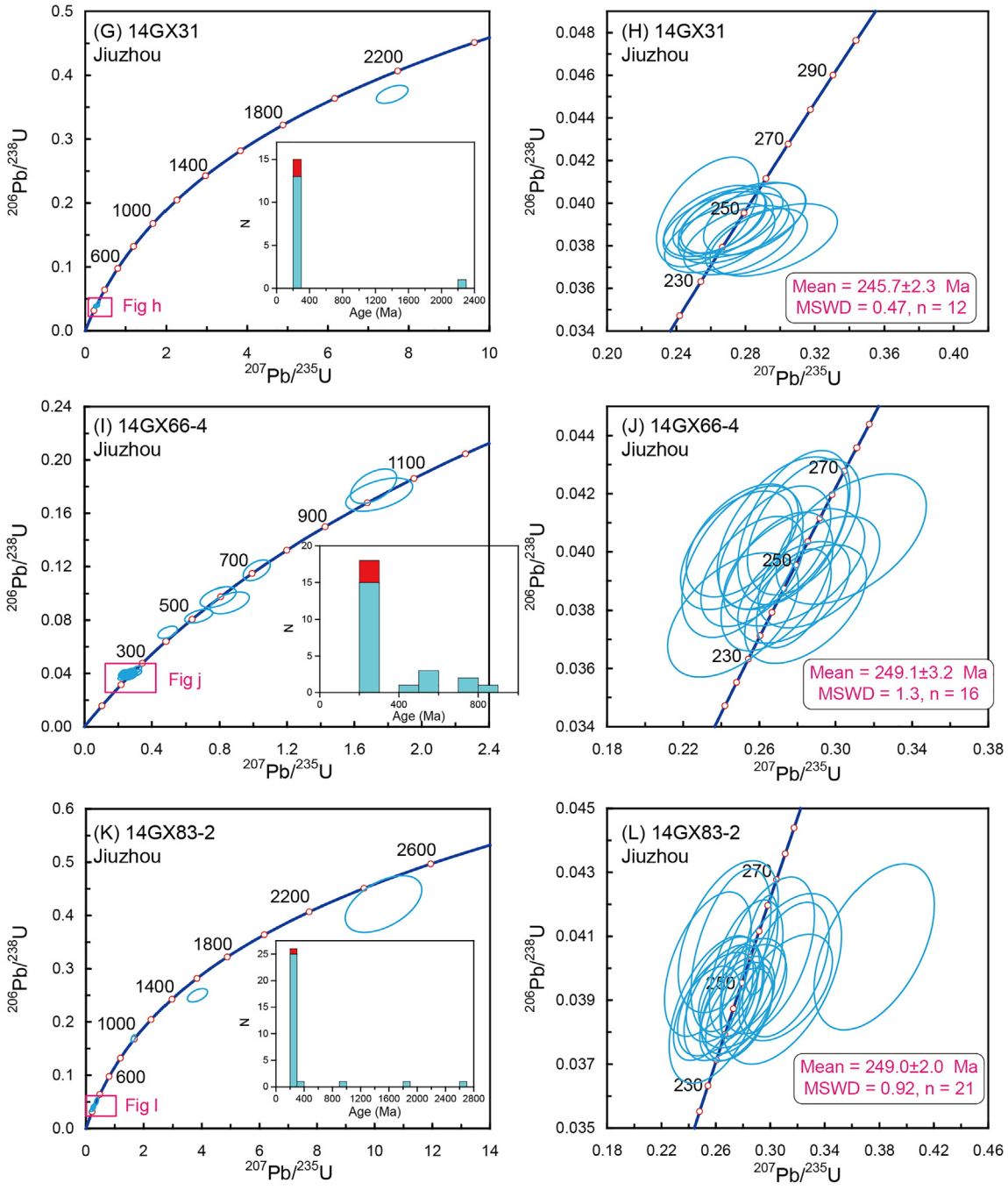

Fig. 4 (*continued*).

Range and the Darongshan batholith were derived from partial melting of sedimentary rocks (e.g., Gao et al., 2014, 2016a; Jiao et al., 2015; Zhao et al., 2015). However, the exact age of parental rocks that were chemically weathered to form these sedimentary rocks are poorly defined.

The previous understanding of source rock ages was mainly relied on whole-rock Nd model ages and zircon Hf model ages (e.g., Chen et al., 2012; Chen and Jahn, 1998; Deng et al., 2004; Gao et al., 2014; Jiao et al., 2015; Qi et al., 2007; Song et al., 2016; Wang et al., 2007a; Zhao et al., 2013, 2015), which are actually indirect constraints because the reworked crust may be juvenile or ancient. For example, many studies consider that the Triassic granites in South China were derived from partial melting of Paleoproterozoic crustal rocks in terms of their Nd and Hf model ages. However, it is inappropriate to equal the Nd-Hf model ages to the formation ages of crustal sources, unless the Paleoproterozoic crust is of juvenile origin and thus derived from decompressional melting of the contemporaneous asthenospheric mantle. Even if this is the case, the model ages are often 100–200 Myr older than the time of juvenile crust growth (Dhuime et al., 2011). If the Paleoproterozoic rocks were reworked from more ancient crust, they would exhibit more ancient model ages. In this regard, the Paleoproterozoic model ages for Triassic granites suggest that their source rocks would originally form not earlier than the Paleoproterozoic. As a matter of fact, Paleoproterozoic magmatic rocks are very limited in South China (Fig. 1; Zhang and Zheng, 2013; Zheng et al., 2013). Many of them show negative $\varepsilon_{Nd}(t)$ and $\varepsilon_{Hf}(t)$ values (e.g., Chen and Jahn, 1998; Zhang and Zheng, 2013), indicating their derivation from

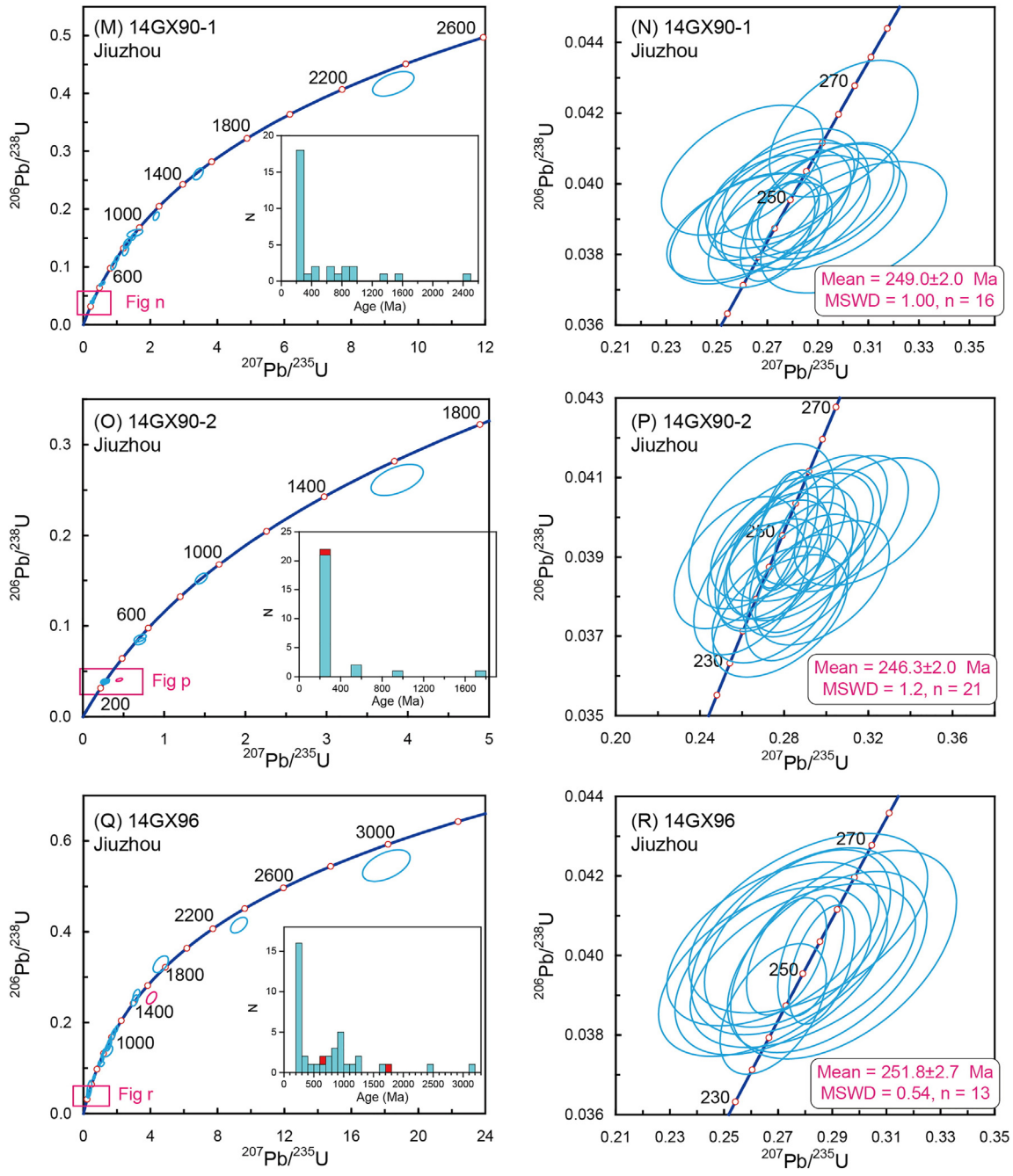

Fig. 4 (*continued*).

reworking of the more ancient crust. Only some of them have positive $\varepsilon_{Hf}(t)$ values (e.g., Wu et al., 2006; Zheng et al., 2006), suggesting their derivation from reworking of the juvenile crust.

In contrast, relict zircons in granites provide a temporal link to their source rocks that cannot be directly observed at present in most cases. Since relict zircons in S-type granites are abundant relative to I- or A-type granites, their role is more significant in the origin of S-type granites (e.g., Gao et al., 2016a; Jeon et al., 2014; Villaros et al., 2012). However, this link must be made on the basis of a correct discrimination between different origins of relict zircons. Only source-derived relict zircons can provide a valuable means in tracing the source rocks of granites (e.g., Villaros et al., 2012) and the history of crustal reworking (e.g., Jeon et al., 2014), as well as in distinguishing true S-type granites from those peraluminous I-type granites (Gao et al., 2016a). Some relict zircons can be produced by tectonothermal events after deposition of the weathered products from source rocks, and they belong to metamorphic or peritectic zircons rather than magmatic zircon in their origin (Chen and Zheng, 2017). Nevertheless, they may provide additional information on the metamorphic and anatectic histories of the source rocks. In comparison, xenocryst zircons trapped by wallrock contamination during emplacement of granitic magmas have nothing to do with the nature of source rocks.

A number of zircon U-Pb geochronological studies have reported the presence of relict zircons in Triassic granites from South China (e.g., Chen et al., 2011; Fu et al., 2015; Gao et al., 2016a; Jiao et al., 2015; Qiao et al., 2015; Song et al., 2016). Although U-Pb ages for these relict zircons were not discussed in detail, they can be collectively categorized into two groups. One is in the Early to Middle

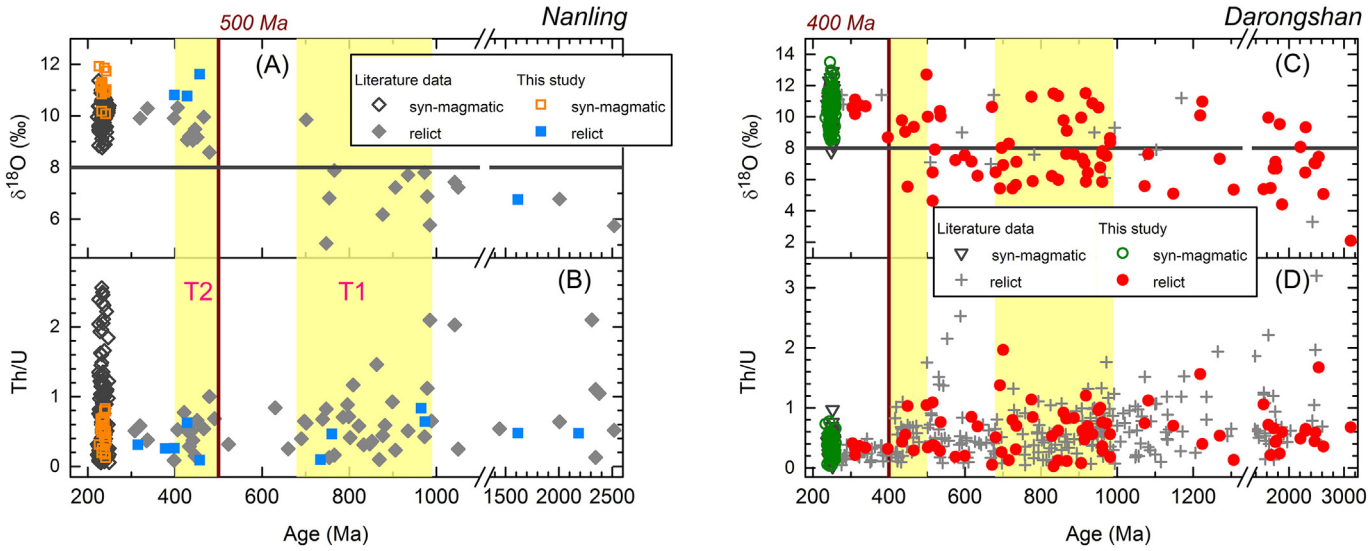

Fig. 5. Plots of zircon O isotope and Th/U ratios against U-Pb ages for Triassic granites in the Nanling Range (left) and the Darongshan area (right). Data sources: Nanling - Gao et al. (2016a), Darongshan - Jiao et al. (2015) and Qiao et al. (2015). Yellow bands represent the ages of Neoproterozoic igneous rocks (T1: 679–990 Ma, Zhang and Zheng, 2013) and the Paleozoic granites (T2: 400–500 Ma, Wang et al., 2013). Red lines labeled with ages denote the beginning of the transient anatexis.

Neoproterozoic and the other is in the Early Paleozoic. The former can be linked to tectonic events for subduction magmatism in the Early Neoproterozoic and rifting magmatism in the Middle Neoproterozoic (Zhang and Zheng, 2013), and the latter is contemporaneous with intracontinental orogenesis in the Early Paleozoic (e.g., Z.X. Li et al., 2010; Wang et al., 2011, 2013). However, most reported U-Pb ages for the relict zircons are relatively scarce for single pluton, and there are no geochemical data having been analyzed at the same time. Nevertheless, it is exceptional in two case studies. One is the zirconological study of Triassic Guidong granites, for which a systematic dataset of zircon U-Pb age, O isotope and trace element were reported (Gao et al., 2016a). The other is the zircon U-Pb geochronological study of the Triassic Darongshan batholith, for which abundant dates are available (Qiao et al., 2015). The majority of relict zircon were not analyzed for their geochemical composition, limiting our understanding of the origin of relict zircons and their geological significance.

Precambrian basement rocks in South China are mainly composed of Neoproterozoic magmatic rocks (Fig. 1), which are widely distributed in

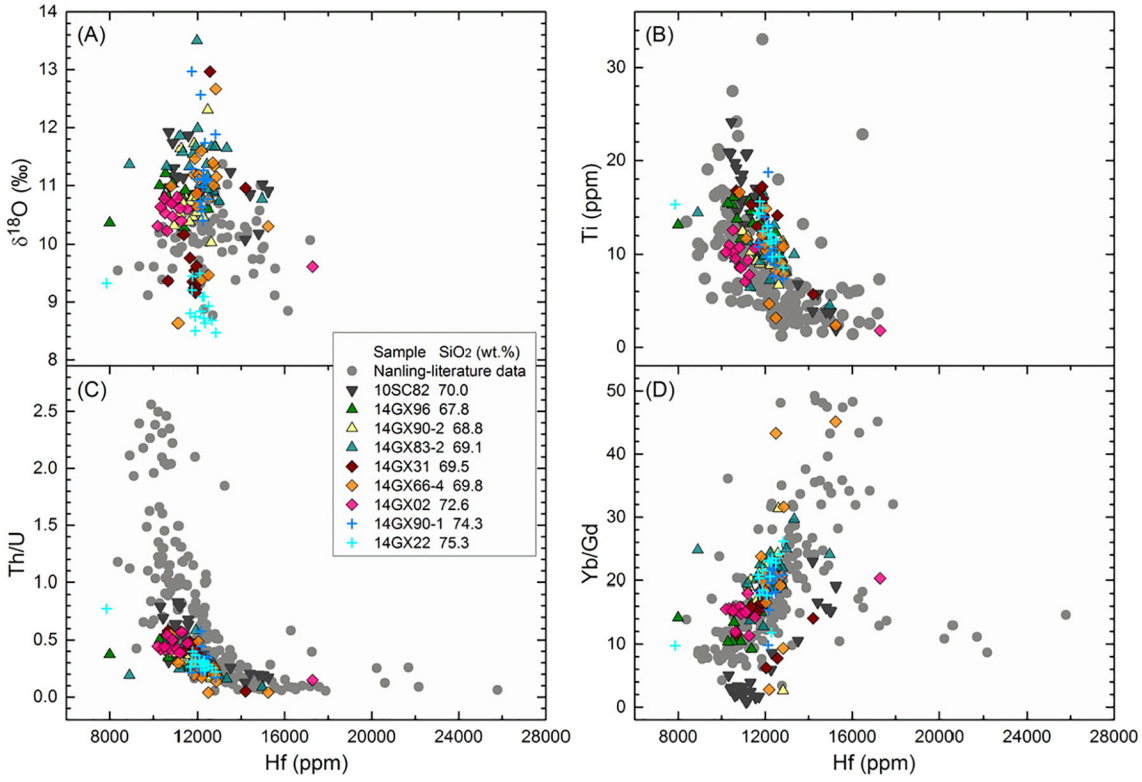

Fig. 6. Plots of zircon Hf content against O isotope and trace element content and ratio for Triassic granites in the Nanling Range and the Darongshan area. Nanling literature data are from Gao et al. (2016a). Data with extremely high Ti contents, possibly due to Ti-rich inclusions, are omitted in (B).

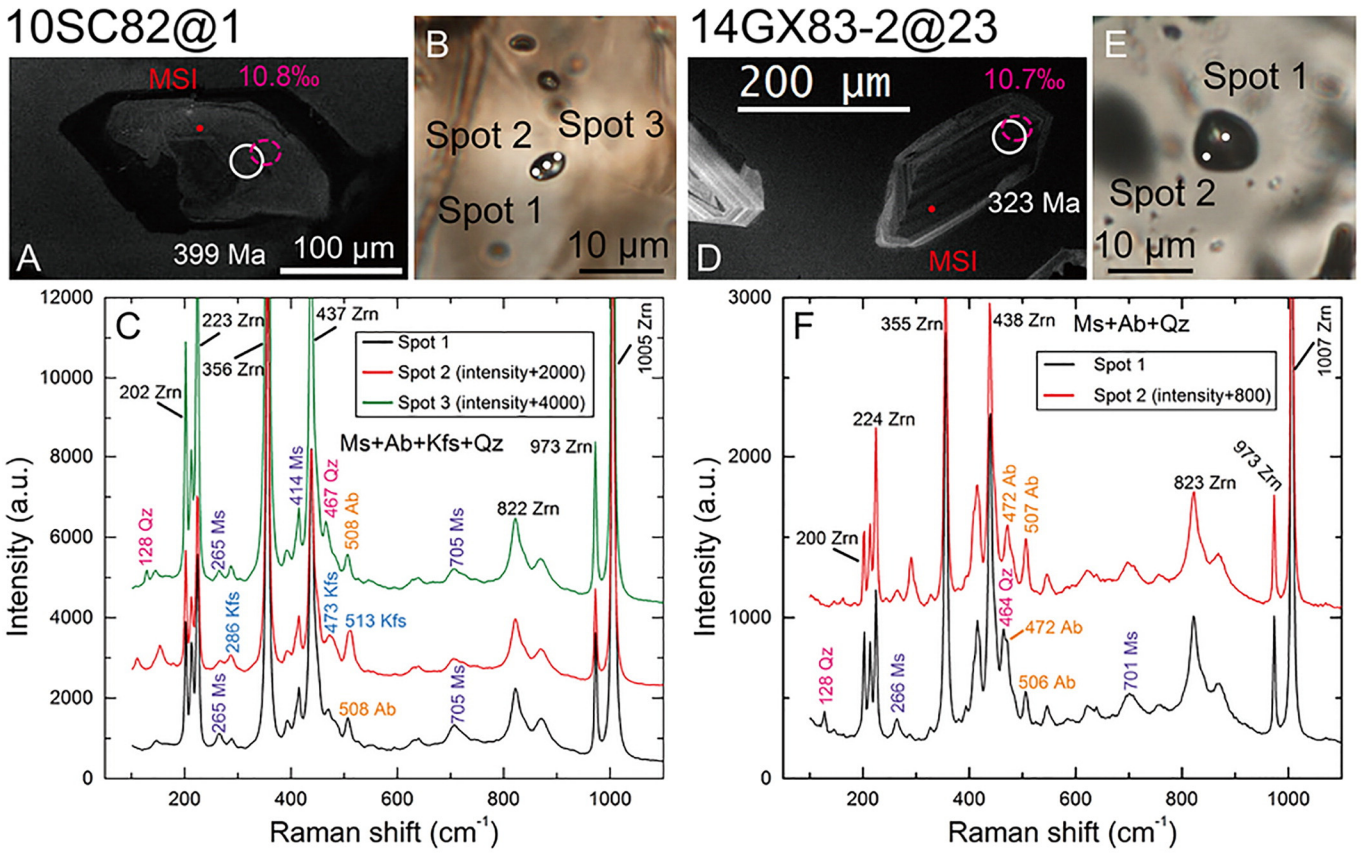

Fig. 7. Identification of multiphase solid inclusions (MSI) in two representative peritectic zircons from the Triassic granites of the southern Zhuguangshan complex (10SC82) and the Jiuzhou pluton (14GX83-2). (A) and (D): CL images with analytical positions of U-Pb isotopes (white circles) and O isotopes (red ellipses). U-Pb ages and $\delta^{18}O$ values as well as the positions of MSI (red dots) are also labeled. (B) and (E): microscopic images of the MSI within zircons under plane polarized light. Spot numbers denote laser Raman analyses. (C) Laser Raman spectra of the MSI in (A), consisting of muscovite (Ms) + albite (Ab) + K-feldspar (Kfs) + quartz (Qz). (F) Laser Raman spectra of the MSI in (D), consisting of Ms + Ab + Qz. Mineral abbreviations are after Whitney and Evans (2010).

the western Cathaysia terrane, the Jiangnan orogen, the Panxi-Hannan orogen between the Yangtze craton and the Tibet block, and the Qinling-Tongbai-Hong'an-Dabie-Sulu orogenic belt between the Yangtze craton and the North China craton (Zheng et al., 2013). These Neoproterozoic magmatic rocks have formed in a long period of 680–990 Ma (Zhang and Zheng, 2013). The western Cathaysia terrane and the Jiangnan orogen, where Triassic granites are exposed, are dominated by lower Neoproterozoic metamorphosed volcanosedimentary strata that were intruded by Middle Neoproterozoic peraluminous (S-type) granites and unconformably overlain by Middle Neoproterozoic weakly metamorphosed strata and upper Neoproterozoic unmetamorphosed Sinian cover (Zhang and Zheng, 2013). Only a few volcanosedimentary successions underwent regional metamorphism at greenschist to lower amphibolite-facies. High-precision zircon U-Pb dating of these metamorphic rocks yields Early to Middle Neoproterozoic ages of ca. 840–990 Ma for their protoliths (Z.X. Li et al., 2010; Yao et al., 2011). Volcanic rocks from these Neoproterozoic strata are predominantly composed of basalts and rhyolites, with minor andesites and dacites, some of which exhibit arc-like geochemical compositions. The Neoproterozoic magmatic rocks have registered both crustal growth and reworking, which is indicated by their Hf model ages ranging from 700 Ma to 3300 Ma with the majority in two ranges of 800–1400 Ma and 1800–2300 Ma (Zhang and Zheng, 2013). Therefore, it is crucial to track reworking of the Neoproterozoic rocks in the origin of Triassic granites. Relict zircons in the Triassic S-type granites have the advantage over the common Nd-Hf isotope compositions for this purpose.

5.2. Relict zircons trace reworking of Neoproterozoic crustal rocks

Relict zircons obtained in this study show highly variable U-Pb ages from 315 ± 5 Ma to 2185 ± 64 Ma for the southern Zhuguangshan granites, and from 304 ± 16 Ma to 3121 ± 30 Ma for the Jiuzhou granites (Table S2). These ages form two main peaks, one in the range of 300–500 Ma in the Paleozoic and the other in the range of 700–1000 Ma in the Neoproterozoic (Fig. 5). Although Th/U ratios for the Neoproterozoic relict zircons are also highly variable (Table S2), they are generally higher than 0.1 (Fig. 5). In addition, these zircons show REE patterns similar to those for the Triassic *syn*-magmatic zircons (Fig. 8), with enrichment in HREE but depletion in LREE relative to MREE, negative Eu anomalies and positive Ce anomalies. Such geochemical features indicate that the Neoproterozoic relict zircons were of magmatic origin (Hoskin and Schaltegger, 2003). High $\delta^{18}O$ values (>8‰) for the Triassic zircon, the occurrence of abundant relict zircons and strongly peraluminous lithochemistry unambiguously point out that the Triassic granites were derived from partial melting of the sedimentary rocks, which are primarily derived from chemical weathering of the Neoproterozoic magmatic rocks. The relict zircons of Neoproterozoic U-Pb ages show a much larger range in $\delta^{18}O$ values than the Triassic *syn*-magmatic zircons (Fig. 5a and c). The Neoproterozoic relict zircons in the Nanling granites exhibit less variable $\delta^{18}O$ values, mostly in a small range from 5 to 8‰. In contrast, those in the Darongshan granites show more variable $\delta^{18}O$ values, generally in a large range from 5 to 11‰. This difference is significant,

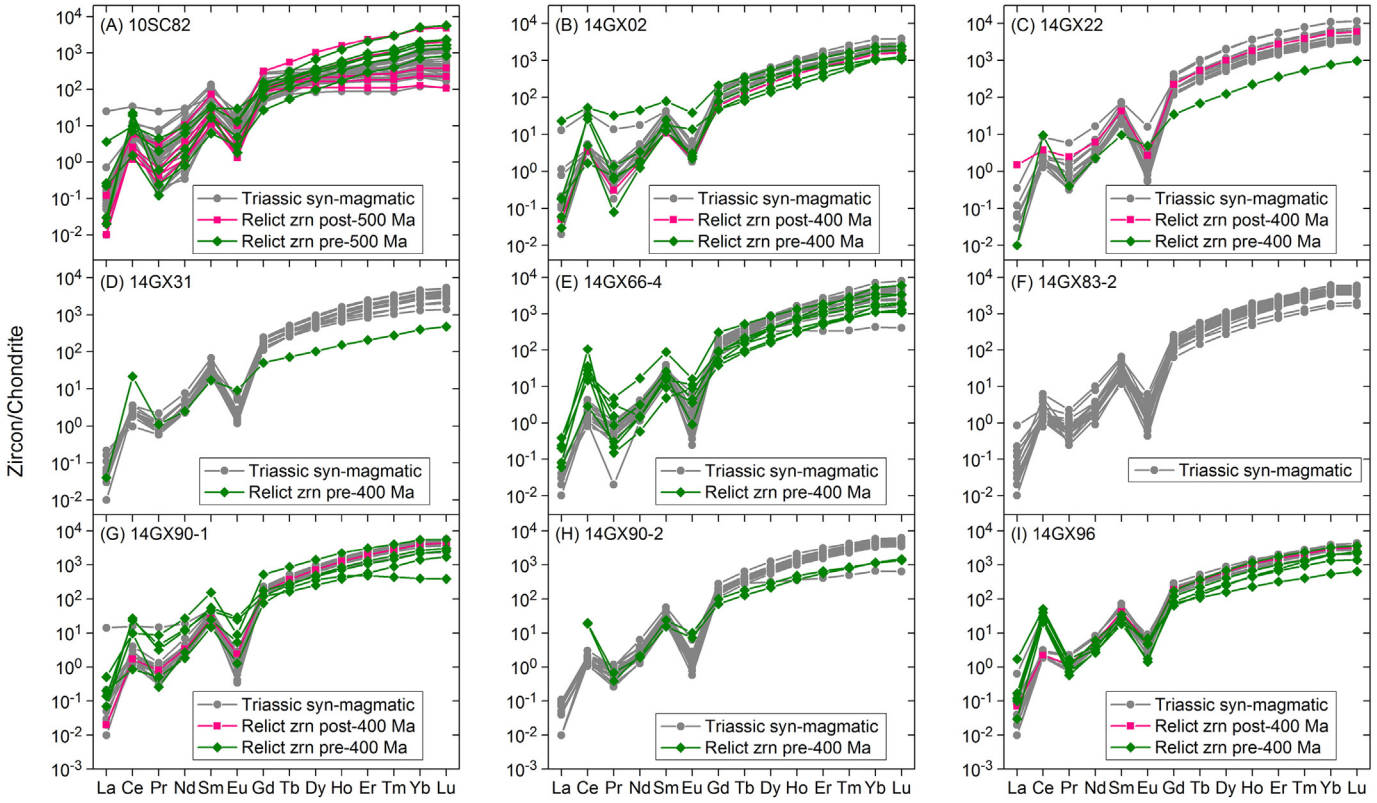

Fig. 8. Plot of chondrite-normalized REE patterns of zircons from the southern Zhuguangshan granites (A) and the Jiuzhou granites (B–I). Normalized values for chondrite are from McDonough and Sun (1995).

indicating that the Neoproterozoic magmatic rocks in the two regions would originate from crustal rocks of different $\delta^{18}O$ values because they experienced chemical weathering of different degrees.

The U-Pb age pattern for Neoproterozoic relict zircons from the Nanling granites are very similar to that for zircons from Upper Neoproterozoic sedimentary rocks in the Nanling Range, which are known to experience metamorphism and anatexis mainly in the Silurian of 420–450 Ma and in the Triassic of 200–250 Ma (e.g., Yu et al., 2008, 2010). In particular, both age patterns exhibit dominant peaks at ca. 750–950 Ma (Fig. 9a, d), overlapping ages for Neoproterozoic magmatic activities in South China (Zhang and Zheng, 2013). However, the zircon U-Pb ages for the Neoproterozoic magmatic rocks in the western Cathaysia terrane and the Jiangnan orogen are dominantly in ca. 800–900 Ma, whereas those for the Neoproterozoic relict zircons in the Triassic granites and the detrital zircons in the Upper Neoproterozoic sedimentary rocks are dominantly in ca. 900–1000 Ma (Fig. 9a, d). This small difference suggests that some of the Neoproterozoic zircon grains in both Triassic granites and Neoproterozoic sedimentary rocks are largely sourced from crustal rocks which are not represented by locally exposed rocks.

For the Triassic granites from the Darongshan batholith, there are plenty of relict zircons with Neoproterozoic U-Pb ages. There is also a dominant peak of U-Pb ages in the Neoproterozoic for detrital zircons in the granulite enclaves of metasedimentary origin (Fig. 10a, b), which are regarded as the source rocks of the Darongshan granites (e.g., Jiao et al., 2013; Zhao et al., 2012). This indicates a significant contribution of the Neoproterozoic crustal rocks to the source of the Darongshan granites. However, the Neoproterozoic sedimentary rocks may not represent the sole source of the Darongshan granites because the relict zircons from the granites have a population of post-700 Ma ages (Fig. 10a). Such ages are deficient in both the granulite enclaves (Fig. 10b; Zhao et al., 2010) and the Upper Neoproterozoic metasedimentary rocks (Fig. 10e; Wan et al., 2010; Yu et al., 2010) from the Yunkai mountains adjacent to the Darongshan batholith (Fig. 1). Instead, the post-700 Ma zircon grains can be found in Permian sedimentary rocks from the Shiwandashan basin (Fig. 10b; Hu et al., 2015), where the Darongshan granites are exposed nearby (Fig. 1). The detrital zircons from the Shiwandashan and Yunkai areas adjacent to the Darongshan area are selected for comparison because there are rare detrital zircon data for rocks in the Darongshan area. In addition, many studies have established that sedimentary environments before the Triassic and the Early Paleozoic orogenesis, respectively, are relatively stable for the three areas, and therefore the Ordovician and Permian sedimentary rocks can be respectively used to represent the averages of the exposed crustal rocks which were weathered before the onset of these orogenesis for the three areas (e.g., Shu, 2012; Yao et al., 2015). The comparison given above suggests that Late Paleozoic sedimentary rocks could have contributed to the source rocks of Triassic granites in addition to the major contribution from the Neoproterozoic magmatic rocks.

Although reworking of the Neoproterozoic rocks was mentioned for the origin of Triassic granites in South China (e.g., Chen et al., 2011; Fu et al., 2015; Gao et al., 2016a; Jiao et al., 2015; Qiao et al., 2015; Song et al., 2016), less attention has been paid to the inheritance of Neoproterozoic zircon U-Pb ages from source rocks. Fu et al. (2015) report a substantial amount of relict zircons with Neoproterozoic U-Pb ages of 627 ± 9 to 992 ± 12 Ma in three Triassic granite plutons from central Hunan (the Xuefeng domain in Fig. 1a), but no detailed discussion was devoted to these old ages for source inheritance. The present study has made a collection of relict zircon U-Pb dates for the Triassic granites in South China (Fig. 11). These dates include not only those relatively plentiful analyses as mentioned above but also those relatively sporadic analyses as acquired in this study. The histograms of these dates show prominent peaks in the Neoproterozoic for most Triassic granites in South China, including those from the Nanling Range, the Darongshan batholith and the Xuefeng domain. The age peak in the

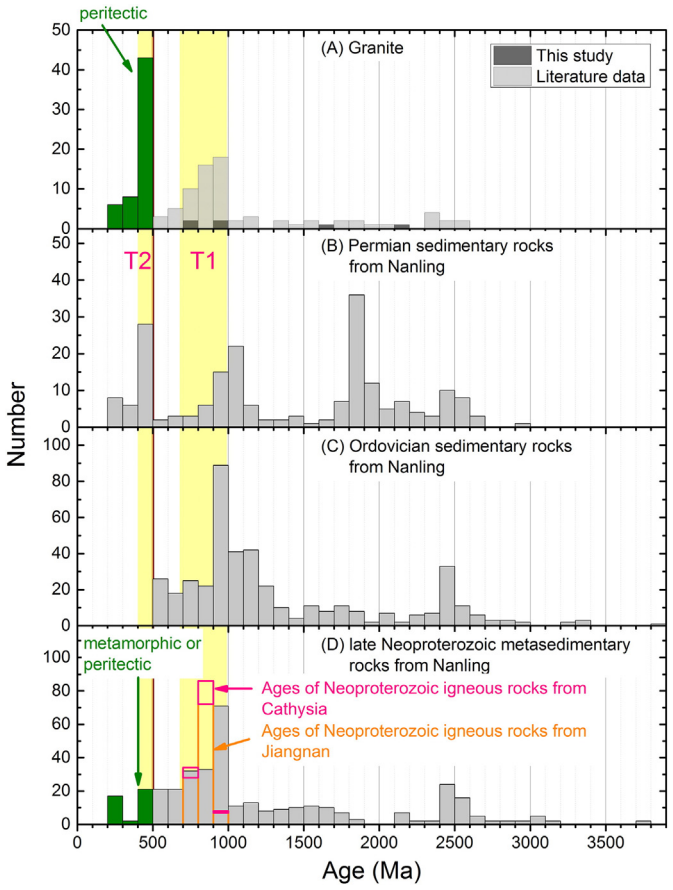

Fig. 9. Histogram of the U-Pb ages for relict zircons from the Nanling granites (A; Zheng and Guo, 2012; Gao et al., 2016a; Song et al., 2016), detrital zircons in the Permian sedimentary rocks from the Nanling Range (B; Li et al., 2012), detrital zircons in the Ordovician sedimentary rocks from the Nanling Range (C; Yao et al., 2011), and zircons in the Late Neoproterozoic metasedimentary rocks from the Nanling Range (D; Yu et al., 2008, 2010). Yellow bands marked with T1 and T2 are the same as those in Fig. 5. Green symbols in (A) are the peritectic zircons, and in (D) are representative of the metamorphic or peritectic zircons. Data sources for the Neoproterozoic igneous rocks from the Jiangnan orogen and the Cathaysia terrane are from Zhang and Zheng (2013) and references therein.

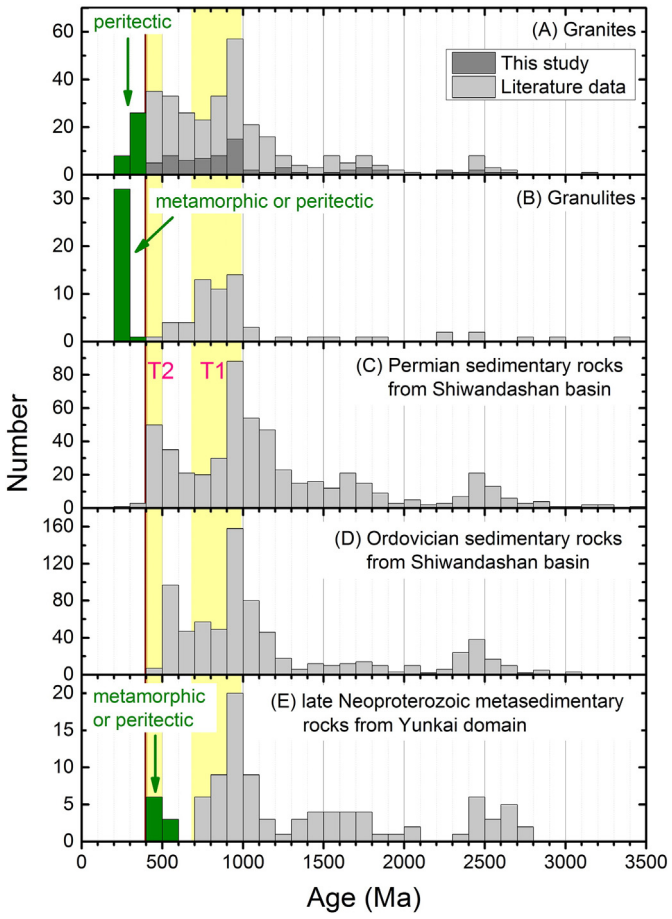

Fig. 10. Histogram of the U-Pb ages for relict zircons from the Darongshan granites (A; Deng et al., 2004; Chen et al., 2011; Jiao et al., 2015; Qiao et al., 2015), zircons from granulite enclaves hosted by the Darongshan granites (B; Zhao et al., 2010), detrital zircons in the Permian sedimentary rocks from the Shiwandashan basin (C; Hu et al., 2015), detrital zircons in the Ordovician sedimentary rocks from the Shiwandashan basin (D; Yao et al., 2015), and zircons in the Late Neoproterozoic metasedimentary rocks from the Yunkai domain (E; Wan et al., 2010; Yu et al., 2010). Yellow bands marked with T1 and T2 are the same as those in Fig. 5. Green symbols in (A) are the peritectic zircons, and in (B) and (E) are representative of the metamorphic or peritectic zircons.

range of 700–1000 Ma is a striking one for the all Triassic granites from all the three areas (Fig. 11). Therefore, in is confident to conclude that reworking of the Neoproterozoic magmatic rocks is the primary mechanism for the origin of Triassic granites in South China. Although it is hard to determine the exact time when these Neoproterozoic rocks were weathered and deposited to form the sedimentary rocks in South China, potential tectonic settings for crustal weathering and deposition are the arc-continent collision orogeny at 830–800 Ma and the continental rifting at 780–740 Ma (Zhang and Zheng, 2013; Zheng et al., 2013).

6. The origin of Paleozoic relict zircons in the Triassic granites

6.1. Petrochronological constraints

Taken previously published data together with our newly reported data, Paleozoic U-Pb ages are considerable for relict zircons in the Triassic S-type granites from South China. The majority of Paleozoic relict zircons show consistently high $\delta^{18}O$ values, similar to those for the Triassic *syn*-magmatic zircons but different from those for the Neoproterozoic relict zircons. In detail, $\delta^{18}O$ values for the Paleozoic relict zircons in the Nanling granites exhibit $\delta^{18}O$ values of 8.6 to 11.6‰, similar to those of 8.8 to 11.9‰ for the Triassic *syn*-magmatic zircons; those from the Darongshan granites show $\delta^{18}O$ values of 8.7 to 11.4‰, similar to those of 7.8 to 13.5‰ for the Triassic *syn*-magmatic zircons. However, there are large variations in their Th/U ratios, which vary from 0.09 to 2.1 in Nanling and from 0.03 to 3.2 in Darongshan.

Because the Paleozoic relict zircons have intermediate U-Pb ages between the Neoproterozoic and Triassic, there are a number of possible interpretations for them. These include: (1) mixing of analytical results; (2) detrital grains; (3) xenocrysts from wallrocks; (4) older relict zircons that suffered Pb loss in later thermal events; (5) metamorphic zircons; and (6) peritectic zircons. The mixed analytical results can be precluded for two reasons: (a) these zircons are individual grains or rimmed by the Triassic domains (Fig. 2), and no single grain with both Triassic rims and multiple generations of older cores has been observed; (b) the analyses are carefully guided by CL images, and the chemical compositions of these zircons are not intermediate between those of the Triassic zircons and the older ones. The origin of detrital grains is also disfavored because the Paleozoic detrital zircons have rarely been observed in the Permian sedimentary rocks from the Shiwandashan basin (Fig. 10; Hu et al., 2015), adjacent to the Darongshan batholith (Fig. 1). Although the Paleozoic detrital zircons can be found in the Permian sedimentary rocks from the Nanling Range (Fig. 9b; Li et al.,

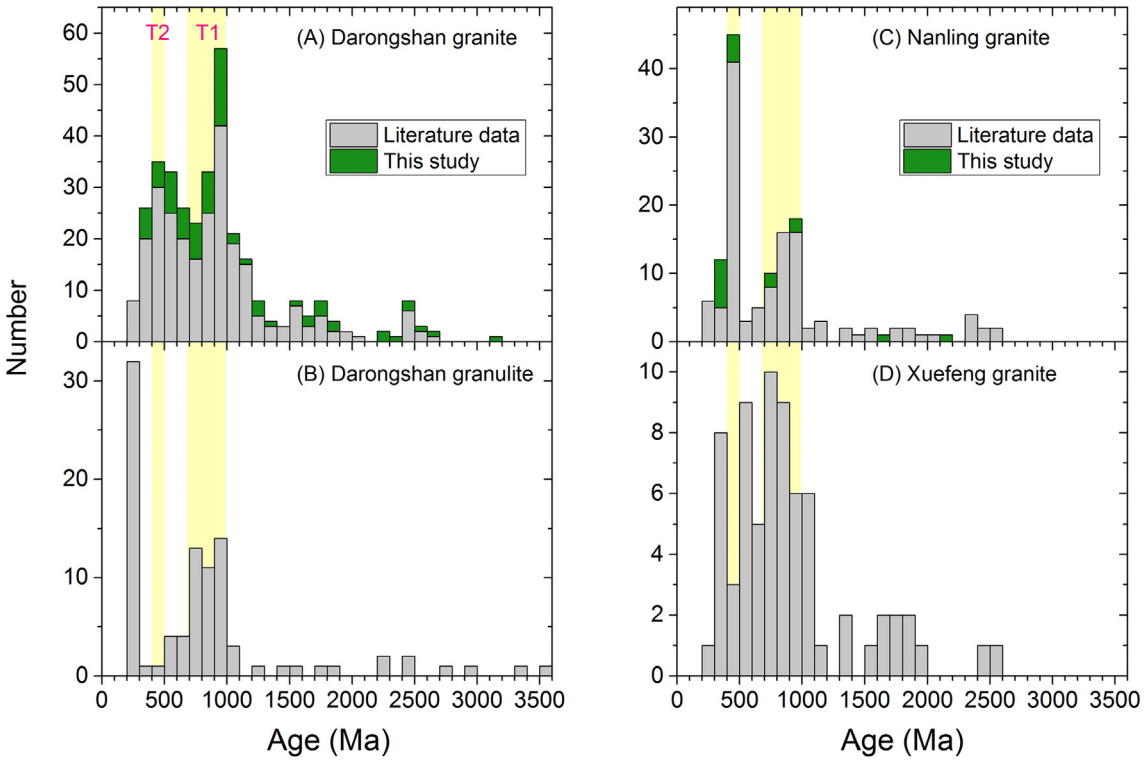

Fig. 11. Histograms of the U-Pb ages for relict zircons from Triassic granites in the Darongshan batholith (A), the Nanling Range (C), and the Xuefeng domain (D). Also shown is histogram of detrital zircons from granulite enclaves hosted in the Darongshan granites (B) as a comparison. Data sources: A-similar to those in Fig. 10a; B-similar to those in Fig. 10b; C-similar to those in Fig. 9a; D-Wang et al., 2007a; Fu et al., 2015.

2012), the Paleoproterozoic detrital grains are also common in these sedimentary rocks but they are rarely detected in the Precambrian zircons of the Triassic granites from Nanling (Fig. 9a).

The interpretation of xenocryst zircon from wallrock contamination is questionable because there is no appropriate crust in the target area that is responsible for the occurrence of Paleozoic relict zircons in the Darongshan and Nanling granites (Figs. 9 and 10). It is well known that South China experienced two strongly tectonothermal events, respectively, in the Silurian (mainly at ca. 420–450 Ma) and in the Triassic (ca. 200–250 Ma), leading to two episodes of pre-Jurassic intracontinental orogenesis in the Phanerozoic (e.g., Z.X. Li et al., 2010; Wang et al., 2013). A lot of studies have established that sedimentary environments before these two episodes of orogeny are relatively stable, and therefore the Ordovician and Permian sedimentary rocks can be used to represent the averages of the exposed crustal rocks which were weathered before the onset of these two orogenesis (e.g., Shu, 2012; Wang et al., 2013; Yao et al., 2015). However, detrital zircon U-Pb age patterns for the Ordovician and Permian sedimentary rocks do not match those for the relict zircons from the Triassic granites (Figs. 9 and 10). Furthermore, rare xenoliths have been found in the Nanling granites (e.g., Chen et al., 2012; Deng et al., 2012; Gao et al., 2014, 2016a, 2016b; Zhao et al., 2015). While some xenoliths can be seen in the Jiuzhou granites, they often show clear shapes implying little influence by the host granites. In addition, whole-rock SiO_2 concentrations are not correlated with zircon $\delta^{18}O$ values (Fig. 12b), suggesting insignificant influence from the wallrock contamination unless the source rocks and the contaminated wallrocks have indistinguishable O isotope compositions. In fact, the wallrock contamination requires high temperatures for its anatexis during magma emplacement, which is generally impeded by the huge energy loss, rapid and substantial crystallization, and stagnation of magma movement (e.g., Clemens and Stevens, 2012). In this regard, all relict zircons in this study are inherited from their source rocks. They can be termed as inherited zircons in general (Chen and Zheng, 2017; Miller et al., 2007).

The inherited zircons may experience variable degrees of Pb loss during granitic magmatism, leading to partial resetting of their U-Pb ages. The resulted zircons may have concordant U-Pb ages if the time difference between the zircon growth and reworking is short, for instance, a Permian zircon grain experiencing Pb loss in the Triassic. On the other hand, they may have discordant U-Pb ages due to significant Pb loss. If the inherited zircons could suffer complete Pb loss, they would give nearly concordant ages close to the timing of the tectonothermal event. However, the interpretation of Pb loss cannot account for the consistently lower Th/U ratios and higher $\delta^{18}O$ values for the second group of young relict zircons whereas the older relict zircons show both highly variable Th/U ratios and $\delta^{18}O$ values (Fig. 5). In addition, the granulite enclaves in the Jiuzhou granite rarely contain zircon grains with concordant U-Pb ages of 300–400 Ma (Fig. 10b; Zhao et al., 2010), but such ages are common in the relict zircons of Triassic granites (Fig. 10a). The granulite enclaves were regarded as an analogue to the source rocks of Triassic granites in the Darongshan batholith in terms of their mineralogy and geochemistry (Jiao et al., 2013; Zhao et al., 2012), but they would have underwent extraction of granitic melts under the granulite-facies conditions (Zheng and Chen, 2017). Therefore, although the Pb loss would inevitably happen, this effect is negligible on the U-Pb ages of young relict zircons.

The Paleozoic relict zircons cannot be interpreted as metamorphic growth for the following reasons: (1) their Th/U ratios are mostly higher than 0.1 (Fig. 5); (2) the occurrence of crystal inclusions composed of felsic minerals (Fig. 7), indicating that their growth in the presence of granitic melts (Chen et al., 2013); and (3) their REE patterns are mostly consistent with those for the Triassic *syn*-magmatic zircons (Fig. 8), with characteristically steep HREE patterns and negative Eu anomalies. This inference is consistent with the observations on the detrital zircons

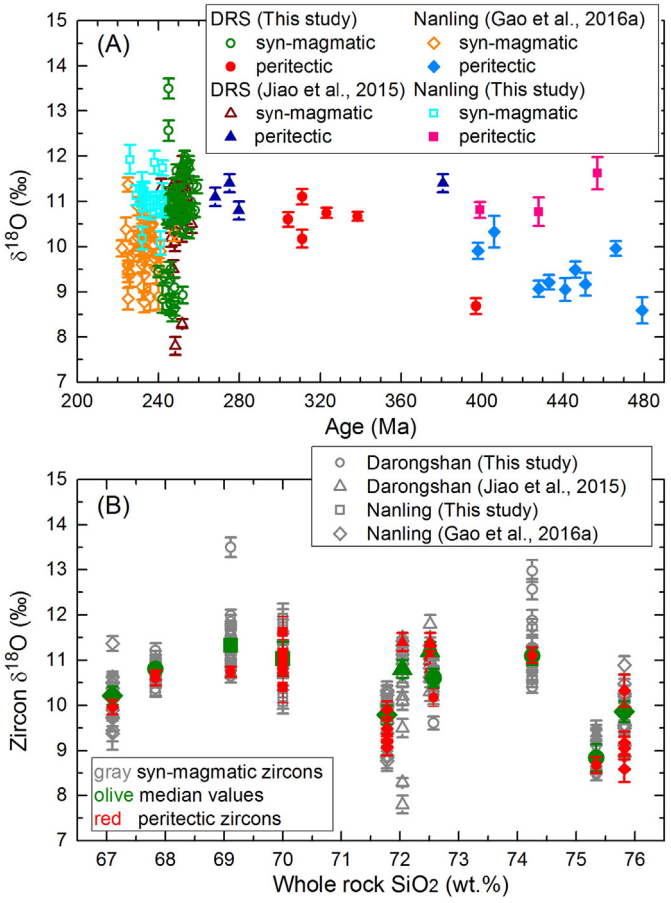

Fig. 12. A: Plot of $\delta^{18}O$ values against U-Pb ages for Triassic magmatic zircons and Paleozoic peritectic zircons. B: Plot of $\delta^{18}O$ value of zircon against SiO_2 content of whole-rock. Error bar is in 2σ. Note that the term of peritectic zircons is used in this study, though they were called relict zircons in the literature.

from sedimentary and metasedimentary rocks in South China, in which rare metamorphic zircons of Paleozoic U-Pb ages can be found (e.g., Wan et al., 2007, 2010; Wang et al., 2007b; Xu et al., 2007; Yu et al., 2008, 2010; Yao et al., 2011, 2015; Li et al., 2012; Hu et al., 2015).

The high $\delta^{18}O$ values for the Paleozoic relict zircons indicate that they would have grown from crustal rocks that have high $\delta^{18}O$ values. Such rocks are most probably the sedimentary rocks that experienced chemical weathering on the surface (Hoefs, 2015). The similarity in $\delta^{18}O$ values between these young relict zircons and the Triassic *syn*-magmatic zircons is coherent in individual samples (Fig. 12a), indicating that these two groups of zircons share common sources. In this regard, the Paleozoic relict zircons are best interpreted as peritectic zircons which were produced by transient melting of the host rocks. Only under such temperatures the crustal rocks could experience transient melting to produce rare peritectic minerals (Chen and Zheng, 2017).

It is known for a long time that zircon may precipitate from magmatic melts during their evolution with significant crystallization of Zr-poor minerals. On the other hand, zircon may grow either through metamorphic reactions at temperatures below the solidus of crustal rocks or through peritectic reactions at temperatures on and above the solidus of crustal rocks (Chen and Zheng, 2017). Zirconium could be provided by the breakdown of Zr-bearing minerals such as biotite and ilmenite (Zheng, 2012), or by the dissolution of protolith zircon (Bea et al., 2006). Peritectic zircons commonly occur in granulites, migmatites and granites (Liu et al., 2012; Chen et al., 2013). Because of the very low Zr abundances in anatectic melts that have not separated from their parental rocks, zircon is not capable of growth directly from the anatectic melts unless the anatectic melts have evolved to high extent with fractional crystallization of Zr-poor minerals from them (Chen and Zheng, 2017). In this case, the anatectic melts have evolved into magmatic melts from which zircons are able to grow due to local Zr oversaturation.

The composition of peritectic zircons is dictated not only by metamorphic P-T conditions but also by the activity of coexisting minerals. Their Th/U ratios may be higher or lower than 0.1, which are primarily dictated by the stability of Th-rich minerals such as allanite and monazite during partial melting (Zheng et al., 2011). They may show low Th/U ratios due to the stability of such minerals during dehydration reactions, but high Th/U ratios due to the breakdown of such minerals. The peritectic zircons in the present study exhibit large variations in CL structure from unzoning to oscillatory zoning, in Th/U ratios from <0.1 to >1.0, in REE abundances from low to high, in HREE patterns from flat to steep, and in Eu anomalies from none to negative. These variations are primarily dictated by the temperature and duration of crustal anataxis. In general, the higher the anatectic temperature, the higher the Th/U ratios; the longer the anatectic duration, the better the oscillatory zoning. Incipient melting at the temperatures on and slightly above the solidus tends to produce low Th/U zircons, whereas transient melting at the temperatures significantly above the solidus tends to produce high Th/U zircons.

Although the Paleozoic relict zircons are scarce in the Triassic granites (generally ca. 1% in individual samples), they indicate considerable influence by thermal pulses on the metasedimentary rocks before their intensive melting for granitic magmatism in the Triassic. As illustrated in Fig. 5, they show highly variable Th/U ratios (0.09–2.1 for the Nanling granites, and 0.03–3.2 for the Darongshan granites) relative to the *syn*-magmatic zircons (0.06–2.6 for the Nanling granites, and 0.03–1.0 for the Darongshan granites) and the Precambrian relict zircons (0.1–2.1 for the Nanling granites, and 0.1–3.2 for the Darongshan granites). This suggests that the anatectic temperatures were highly variable and Th-rich accessory minerals were variably broken down during transient melting. Therefore, these Paleozoic relict zircons are primarily not of detrital origin, and their occurrence in granites provides an additional means to unravel the history of crustal anataxis before the granitic magmatism.

6.2. Insights into the history of crustal anatexis

The composition of granites is complicated because they are composed of magmatic, peritectic and residual minerals in different proportions, depending on the P-T conditions of crustal anatexis. In general, the granites of sedimentary sources (S-type) contain larger amounts of peritectic and residual minerals than the granites of igneous sources (I-type). For this reason, minerals in S-type granites commonly show larger variations in composition than minerals in I-type granites. In particular, peritectic minerals generally exhibit highly variable compositions because their growth through different types of peritectic reaction at different P-T conditions. In contrast, magmatic minerals may show relatively homogenous geochemistry because their crystallization from the magmatic melts of relatively homogenized composition. As such, it is important to discriminate between peritectic and magmatic minerals in granites when dealing with their petrogenesis.

Zircon is a very refractory mineral and thus has the capacity to record the primary signature of its growth. The abundance of incompatible trace elements in zircon can be used in tracing its origin. It is known that U is a water-soluble element and thus susceptible to transport during metamorphic dehydration at temperatures below the solidus of crustal rocks. In contrast, Th is a water-insoluble element but melt-mobile one and hence susceptible to transport during partial melting at the temperatures above the solidus of crustal rocks. As a consequence, metamorphic zircons generally have lower Th/U ratios than 0.1 whereas magmatic zircons usually have higher Th/U ratios than 0.4. As such, zircon Th/U ratios are often used to discriminate its origins. Peritectic zircons may show highly variable Th/U ratios from <0.1 to

>1.0, depending on the stability of Th-bearing minerals during partial melting. If partial melting takes place at the temperatures on and slightly above the solidus, crustal anataxis is incipient and the peritectic zircons produced are of lower Th/U ratios than 0.1 (Chen and Zheng, 2017). If partial melting takes place at the temperatures profoundly above the solidus, crustal anataxis is significant and the peritectic zircons resulted are of higher Th/U ratios than 0.4. In either case, some peritectic zircons can be characterized by intermediate Th/U ratios between 0.1 and 0.4.

The present study obtains that the *syn*-magmatic zircons of Triassic U-Pb ages from the Nanling granites show a larger range of Th/U ratios from 0.06 to 2.6, and those from the Darongshan granites exhibit a smaller range of Th/U ratios from 0.03 to 1.0 (Figs. 5 and 6). In this regard, those zircons with lower Th/U ratios lower than 0.4 may be of peritectic origin or magmatic origin growing from highly evolved melts. As such, these Triassic zircons consist of magmatic and peritectic ones. On the other hand, the relict zircons of Paloezoic U-Pb ages show highly variable Th/U ratios of 0.09–2.1 for the Nanling granites and 0.03–3.2 for the Darongshan granites. Such variations suggest a large fluctuation in anatectic temperatures. While the low Th/U ratios may be responsible for incipient melting at the temperatures on the solidus, the high Th/U ratios may indicate transient melting at the temperatures significantly above the solidus.

Dehydration of crustal rocks in the lower crust is spatially and temporally coupled with hydration of their overlying rocks in the middle crust, forming the relationship between the source and sink of water (Zheng and Chen, 2017). At low water activities, crustal rocks undergo dehydration melting due to the breakdown of hydrous minerals such as muscovite, biotite and amphibole at higher temperatures. As soon as the water is liberated from the hydrous minerals, it fluxes into the overlying rocks for hydration melting at lower temperatures. Because of the fluctuation in temperature at the Moho of orogenic lithosphere, crustal rocks there may experience local dehydration on the one hand and local hydration on the other hand, resulting in multiple episodes of partial melting at different degrees. Whereas the lower temperatures tend to cause transient melting for local migmatization, the higher temperatures can lead to intensive melting for granitic magmatism. While magmatic zircons are readily utilized in U-Pb dating of magma crystallization, peritectic zircons are amenable to U-Pb dating of migmatization at different degrees.

The Triassic granites from the Nanling Range and the Darongshan batholith show different intervals between the youngest ages of detrital zircons and the oldest ages of peritectic zircons (Fig. 5). The gap lies between 630 Ma and 523 Ma for the Nanling granites, but it is only between 434 Ma and 397 Ma for the Darongshan granites. Such a difference suggests that the tectonic processes from deposition to burial and then to transient melting for the growth of peritectic zircons are discontinuous in the Nanling Range, but they are almost not disrupted in the Darongshan batholith. The transient melting has occurred since ca. 500 Ma and ca. 400 Ma, respectively, for the source rocks of Triassic granites in the Nanling Range and the Darongshan batholith. These two anatectic ages are synchronous with the initial and final ages, respectively, for the Early Paleozoic tectonothermal events in South China (e.g., Z.X. Li et al., 2010; Wang et al., 2013). Therefore, the Triassic granites were produced by reworking of the specific rocks that experienced the transient melting in the Early Paleozoic.

Crustal rock may undergo different degrees of partial melting in orogenic lithosphere, depending on the thermal structure of orogens (Zheng and Chen, 2016, 2017). If they are heated at higher temperatures, intensive melting takes place to produce granites and migmatites. In contrast, there is only transient melting at lower temperatures to produce migmatites with peritectic zircons (Chen and Zheng, 2017). In the Nanling Range, sedimentary rocks were buried for regional metamorphism since ≥500 Ma. It is possible in the Nanling Range that these metasedimentary rocks experienced transient melting in the Paleozoic to generate the peritectic zircons and then underwent intensive anatexis in the Triassic to produce the peraluminous granites. Although the two-stage processes were not underlined before for the Nanling Triassic granites, they have been recorded by a number of petrological and geochemical studies (e.g., Chen et al., 2012; Deng et al., 2012; Gao et al., 2014, 2016a; Shu et al., 2014; Song et al., 2016; Wang et al., 2011; Zhao et al., 2015). The two-stage model is also applicable to the origin of the Darongshan grantites. Neoproterozoic sedimentary rocks there were transported from the surface into the deep crust since ≥400 Ma, when the Early Paleozoic orogenesis came into the end and postorogenic extension started to prevail (e.g., Z.X. Li et al., 2010; Shu, 2012; Wang et al., 2013). Afterwards these rocks suffered the thermal overprinting for transient melting in the period of ca. 400–250 Ma, and then intensive melting for granitic magmatism in the Triassic.

7. Conclusions

The high $\delta^{18}O$ values, peraluminous lithochemistry and the occurrence of plentiful relict zircons in Triassic granites from the Nanling Range and the Darongshan bathlith demonstrate that these granites were derived from partial melting of sedimentary rocks. The relict zircons of Neoproterozoic U-Pb ages are prominent and they are of magmatic origin, indicating that their provenances are Neoproterozoic magmatic rocks. Reworking of the Neoproterozoic crustal rocks is thus responsible for the origin of Triassic granites. This provides a temporal link to the source rocks of granites, refining the previous definition in terms of whole-rock Nd and zircon Hf model ages. In addition, some relict zircons are of Paleozoic U-Pb ages. These zircons show consistently high $\delta^{18}O$ values similar to the Triassic *syn*-magmatic zircons. Thus, they are interpreted as peritectic zircons that grew during the transient melting of metasedimentary rocks before intensive melting for granitic magmatism in the Triassic. Therefore, the U-Pb ages and geochemical compositions of relict zircons are of important value in tracing the source rocks of granites and their anatectic history.

Supplementary data to this article can be found online at https://doi.org/10.1016/j.lithos.2017.11.036.

Acknowledgments

This study was supported by the Nature Science Foundation of China (41473034) and the China Postdoctoral Science Foundation (2016M600486). GP appreciates the generous sharing of sample sites from Dr. Song-Bai Peng (China University of Geosciences, Wuhan) and Dr. Liang Zhao (Guangzhou Institute of Geochemistry, Chinese Academy of Sciences). We are grateful to Qiang He, Wei Rong and Ying-Hui Lu for their assistance with field sampling. This paper benefits greatly from constructive comments by two anonymous reviewers and editorial handling by Dr. Xian-Hua Li.

References

Andersen, T., 2002. Correction of common lead in U-Pb analyses that do not report ^{204}Pb. Chemical Geology 192, 59–79.
Bea, F., Montero, P., Ortega, M., 2006. A LA-ICP-MS evaluation of Zr reservoirs in common crustal rocks: implication for Zr and Hf geochemistry, and zircon-forming process. Canadian Mineralogist 44, 693–714.
Brown, M., 2013. Granite: from genesis to emplacement. Geological Society of America Bulletin 125, 1079–1113.
Chen, J.F., Jahn, B.-M., 1998. Crustal evolution of southeastern China: Nd and Sr isotopic evidence. Tectonophysics 284, 101–133.
Chen, R.-X., Zheng, Y.-F., 2017. Metamorphic zirconology of continental subduction zone. Journal of Asian Earth Sciences 145, 149–176.
Chen, C.H., Hsieh, P.S., Lee, C.Y., Zhou, H.W., 2011. Two episodes of the Indosinian thermal event on the South China Block: constraints from LA-ICPMS U-Pb zircon and electron microprobe monazite ages of the Darongshan S-type granitic suite. Gondwana Research 19, 1008–1023.
Chen, Y.W., Bi, X.W., Hu, R.Z., Dong, S.H., 2012. Element geochemistry, mineralogy, geochronology and zircon Hf isotope of the Luxi and Xiazhuang granites in Guangdong province, China: implications for U mineralization. Lithos 150, 119–134.
Chen, Y.-X., Zheng, Y.-F., Hu, Z.C., 2013. Synexhumation anatexis of ultrahigh-pressure metamorphic rocks: petrological evidence from granitic gneiss in the Sulu orogeny. Lithos 156–159, 69–96.

Claiborne, L.L., Miller, C.F., Wooden, J.L., 2010. Trace element composition of igneous zircon: a thermal and compositional record of the accumulation and evolution of a large silicic batholith, Spirit Mountain, Nevada. Contributions to Mineralogy and Petrology 160, 511–531.
Clemens, J.D., Stevens, G., 2012. What controls chemical variation in granitic magmas? Lithos 134–135, 317–329.
Deng, X.G., Chen, Z.G., Li, X.H., 2004. SHRIMP U-Pb zircon dating of the Darongshan-Shiwandashan. Geological Review 50, 426–432.
Deng, P., Ren, J.S., Ling, H.F., Shen, W.Z., Sun, L.Q., Zhu, B., Tan, Z.Z., 2012. SHRIMP zircon U-Pb ages and tectonic implications for Indosinian granitoids of southern Zhuguangshan granitic composite, South China. Chinese Science Bulletin 57, 1542–1552.
Dhuime, B., Hawkesworth, C., Cawood, P., 2011. When continents formed. Science 331, 154–155.
Fu, S., Hu, R., Bi, X., Chen, Y., Yang, J., Huang, Y., 2015. Origin of Triassic granites in central Hunan Province, South China: constraints from zircon U-Pb ages and Hf and O isotopes. International Geology Review 57, 97–111.
Gao, P., Zhao, Z.-F., Zheng, Y.-F., 2014. Petrogenesis of Triassic granites from the Nanling Range in South China: implications for geochemical diversity in granites. Lithos 210–211, 40–56.
Gao, P., Zheng, Y.-F., Zhao, Z.-F., 2016a. Distinction between S-type and peraluminous I-type granites: zircon versus whole-rock geochemistry. Lithos 258–259, 77–91.
Gao, P., Zhao, Z.-F., Zheng, Y.-F., 2016b. Magma mixing in granite petrogenesis: insights from biotite inclusions in quartz and feldspar of Mesozoic granites from South China. Journal of Asian Earth Sciences 123, 142–161.
Gao, P., Zheng, Y.-F., Zhao, Z.-F., 2017. Triassic granites in South China: a geochemical perspective on their characteristics, petrogenesis, and tectonic significance. Earth-Science Reviews 173, 266–294.
Hoefs, J., 2015. Stable Isotope Geochemistry. 7th edition. Springer Verlag, Berlin Heidelberg (285 pp.).
Hoskin, P.W.O., Schaltegger, U., 2003. The composition of zircon and igneous and metamorphic petrogenesis. Reviews in Mineralogy and Geochemistry 53, 27–62.
Hsieh, P.S., Chen, C.H., Yang, H.J., Lee, C.Y., 2008. Petrogenesis of the Nanling Mountains granites from South China: constraints from systematic apatite geochemistry and whole-rock geochemical and Sr-Nd isotope compositions. Journal of Asian Earth Sciences 33, 428–451.
Hu, L., Cawood, P.A., Du, Y., Xu, Y., Xu, W., Huang, H., 2015. Detrital records for upper Permian-lower Triassic succession in the Shiwandashan basin, South China and implications for Permian-Triassic (Indosinian) orogeny. Journal of Asian Earth Sciences 98, 152–166.
Huang, J.Q., Ren, J.S., Jiang, C.F., Zhang, Z.K., Qin, D.Y., 1987. Geotectonic Evolution of China. Springer-Verlag, Berlin, pp. 1–203.
Jeon, H., Williams, I.S., Bennett, V.C., 2014. Uncoupled O and Hf isotopic systems in zircon from the contrasting granite suites of the New England Orogen, eastern Australia: implications for studies of Phanerozoic magma genesis. Geochimica et Cosmochimica Acta 146, 132–149.
Jiao, S.J., Guo, J.H., Peng, S.B., 2013. Petrogenesis of garnet in the Darongshan-Shiwandashan granitic suite of the South China Block and the metamorphism of the granulite enclave. Acta Petrologica Sinica 29, 1740–1758 (in Chinese with English abstract).
Jiao, S.J., Li, X.H., Huang, H.Q., Deng, X.G., 2015. Metasedimentary melting in the formation of charnockite: petrological and zircon U-Pb-Hf-O isotope evidence from the Darongshan S-type granitic complex in southern China. Lithos 239, 217–233.
Kemp, A.I.S., Hawkesworth, C.J., 2003. Granitic perspectives on the generation and secular evolution of the continental crust. In: Rudnick, R.L. (Ed.), Treatise on Geochemistry, the Crust. Elsevier, Amsterdam, pp. 349–410.
Kemp, A.I.S., Hawkesworth, C.J., Foster, G.L., Paterson, B.A., Woodhead, J.D., Hergt, J.M., Gray, C.M., Whitehouse, M.J., 2007. Magmatic and crustal differentiation history of granitic rocks from Hf-O isotopes in zircon. Science 315, 980–983.
Li, Z.X., Li, X.H., 2007. Formation of the 1300-km-wide intracontinental orogen and postorogenic magmatic province in Mesozoic South China: a flat-slab subduction model. Geology 35, 179–182.
Li, X.H., Li, W.X., Wang, X.C., Li, Q.L., Liu, Y., Tang, G.Q., 2009. Role of mantle-derived magma in genesis of early Yanshanian granites in the Nanling Range, South China: in situ zircon Hf-O isotopic constraints. Science in China Series D: Earth Sciences 52, 1262–1278.
Li, Z.X., Li, X.H., Wartho, J.A., Clark, C., Li, W.X., Zhang, C.L., Bao, C., 2010a. Magmatic and metamorphic events during the early Paleozoic Wuyi-Yunkai orogeny, southeastern South China: new age constraints and pressure-temperature conditions. Geological Society of America Bulletin 122, 772–793.
Li, Q.L., Li, X.H., Liu, Y., Tang, G.Q., Yang, J.H., Zhu, W.G., 2010b. Precise U-Pb and Pb-Pb dating of Phanerozoic baddeleyite by SIMS with oxygen flooding technique. Journal of Analytical Atomic Spectrometry 25, 1107–1113.
Li, X.H., Li, W.X., Li, Q.L., Wang, X.C., Liu, Y., Yang, Y.H., 2010c. Petrogenesis and tectonic significance of the 860 Ma Gangbian alkaline complex in South China: evidence from in situ zircon U-Pb dating, Hf-O isotopes and whole-rock geochemistry. Lithos 114, 1–15.
Li, X.H., Long, W.G., Li, Q.L., Liu, Y., Zheng, Y.F., Yang, Y.H., Chamberlain, K.R., Wan, D.F., Guo, C.H., Wang, X.C., Tao, H., 2010d. Penglai zircon megacrysts: a potential new working reference material for microbeam determination of Hf-O isotopes and U-Pb age. Geostandards and Geoanalytical Research 34, 117–134.
Li, X.H., Li, Z.X., He, B., Li, W.X., Li, Q.L., Gao, Y.Y., Wang, X.C., 2012. The Early Permian active continental margin and crustal growth of the Cathaysia Block: in situ U-Pb, Lu-Hf and O isotope analyses of detrital zircons. Chemical Geology 328, 195–207.
Li, X.H., Tang, G.Q., Gong, B., Yang, Y.H., Hou, K.J., Hu, Z.C., Li, Q.L., Liu, Y., Li, W.X., 2013. Qinghu zircon: a working reference for microbeam analysis of U-Pb age and Hf and O isotopes. Chinese Science Bulletin 58, 4647–4654.
Liu, Y.S., Gao, S., Hu, Z., Gao, C., Zong, K., Wang, D., 2010. Continental and oceanic crust recycling-induced melt-peridotite interactions in the trans-north China Orogen: U-Pb dating, Hf isotopes and trace elements in zircons from mantle xenoliths. Journal of Petrology 51, 537–571.
Liu, F.L., Robinson, P.L., Liu, P.H., 2012. Multistage partial melting events in the Sulu UHP terrane: zircon U-Pb dating of granitic leucosomes within amphibolite and gneiss. Journal of Metamorphic Geology 30, 887–906.
Ludwig, K.R., 2003. User's Manual for Isoplot 3.00: A Geochronological Toolkit for Microsoft Excel. Berkeley Geochronology Center Special Publication, Berkeley 4 (70 pp.).
McDonough, W.F., Sun, S.-S., 1995. The composition of the Earth. Chemical Geology 120, 223–253.
Miller, J.S., Matzel, J.P., Miller, C.F., Burgess, S.D., Miller, R.B., 2007. Zircon growth and recycling during the assembly of large, composite arc plutons. Journal of Volcanology and Geothermal Research 167, 282–299.
Nasdala, L., Hofmeister, W., Norberg, N., Mattinson, J.M., Corfu, F., Dörr, W., Kamo, S.L., Kennedy, A.K., Kronz, A., Reiners, P.W., Frei, D., Kosler, J., Wan, Y., Götze, J., Häger, T., Kröner, A., Valley, J.W., 2008. Zircon M257-a homogeneous natural reference material for the ion microprobe U-Pb analysis of zircon. Geostandards and Geoanalytical Research 32, 47–265.
Qi, C.S., Deng, X.G., Li, W.X., Li, X.H., Yang, Y.H., Xie, L.W., 2007. Origin of the Darongshan-Shiwandashan S-type granitoid belt from southeastern Guangxi: geochemical and Sr-Nd-Hf isotopic constraints. Acta Petrologica Sinica 2, 403–412.
Qiao, L., Wang, Q., Li, C., 2015. The western segment of the suture between the Yangtze and Cathaysia blocks: constraints from inherited and co-magmatic zircons from Permian S-type granitoids in Guangxi, South China. Terra Nova 27, 392–398.
Shu, L.S., 2012. An analysis of principle features of tectonic evolution in South China Block. Geological Bulletin of China 31, 1035–1053 (in Chinese with English abstract).
Shu, L.S., Jahn, B.M., Charvet, J., Santosh, M., Wang, B., Xu, X.S., Jiang, S.Y., 2014. Early Paleozoic depositional environment and intraplate tectono-magmatism in the Cathaysia Block (South China): evidence from stratigraphic, structural, geochemical, and geochronological investigations. American Journal of Science 314, 154–186.
Sláma, J., Košler, J., Condon, D.J., Crowley, J.L., Gerdes, A., Hanchar, J.M., Horstwood, M.S.A., Morris, G.A., Nasdala, L., Norberg, N., Schaltegger, U., Schoene, B., Tubrett, M.N., Whitehouse, M.J., 2008. Plešovice zircon-a new natural reference material for U–Pb and Hf isotopic microanalysis. Chemical Geology 249, 1–35.
Song, M.J., Shu, L.S., Santosh, M., 2016. Early Mesozoic granites in the Nanling Belt, South China: implications for intracontinental tectonics associated with stress regime transformation. Tectonophysics 676, 148–169.
Stacey, J.S., Kramers, J.D., 1975. Approximation of terrestrial lead isotope evolution by a two-stage model. Earth and Planetary Science Letters 26, 207–221.
Villaros, A., Buick, I.S., Stevens, G., 2012. Isotopic variations in S-type granites: an inheritance from a heterogeneous source? Contributions to Mineralogy and Petrology 163, 243–257.
Wan, Y., Liu, D., Xu, M., Zhuang, J., Song, B., Shi, Y., Du, L., 2007. SHRIMP U-Pb zircon geochronology and geochemistry of metavolcanic and metasedimentary rocks in Northwestern Fujian, Cathaysia block, China: tectonic implications and the need to redefine lithostratigraphic units. Gondwana Research 12, 166–183.
Wan, Y., Liu, D., Wilde, S.A., Cao, J., Chen, B., Dong, C., Song, B., Du, L., 2010. Evolution of the Yunkai terrane, South China: evidence from SHRIMP zircon U-Pb dating, geochemistry and Nd isotope. Journal of Asian Earth Sciences 37, 140–153.
Wang, Y.J., Fan, W.M., Sun, M., Liang, X.Q., Zhang, Y.H., Peng, T.P., 2007a. Geochronological, geochemical and geothermal constraints on petrogenesis of the Indosinian peraluminous granites in the South China Block: a case study in the Hunan Province. Lithos 96, 475–502.
Wang, Y.J., Fan, W., Zhao, G., Ji, S., Peng, T.P., 2007b. Zircon U-Pb geochronology of gneissic rocks in the Yunkai massif and its implications on the Caledonian event in the South China Block. Gondwana Research 12, 404–416.
Wang, Y.J., Zhang, A.M., Fan, W.M., Zhao, G.C., Zhang, G.W., Zhang, F.F., Zhang, Y.Z., Li, S.Z., 2011. Kwangsian crustal anatexis within the eastern South China Block: geochemical, zircon U-Pb geochronological and Hf isotopic fingerprints from the gneissoid granites of Wugong and Wuyi-Yunkai Domains. Lithos 127, 239–260.
Wang, Y.J., Fan, W.M., Zhang, G., Zhang, Y., 2013. Phanerozoic tectonics of the South China Block: key observations and controversies. Gondwana Research 23, 1273–1305.
Whitney, D.L., Evans, B.W., 2010. Abbreviations for names of rock-forming minerals. American Mineralogist 95, 185–187.
Wu, R.X., Zheng, Y.F., Wu, Y.B., Zhao, Z.F., Zhang, S.B., Liu, X., Wu, F.Y., 2006. Reworking of juvenile crust: element and isotope evidence from Neoproterozoic granodiorite in South China. Precambrian Research 146, 179–212.
Xu, X.S., O'Reilly, S.Y., Griffin, W.L., Wang, X.L., Pearson, N.J., He, Z.Y., 2007. The crust of Cathaysia: age, assembly and reworking of two terranes. Precambrian Research 158, 51–78.
Yao, J.L., Shu, L.S., Santosh, M., 2011. Detrital zircon U-Pb geochronology, Hf-isotopes and geochemistry-new clues for the Precambrian crustal evolution of Cathaysia Block, South China. Gondwana Research 20, 553–567.
Yao, W.H., Li, Z.X., Li, W.X., Su, L., Yang, J.H., 2015. Detrital provenance evolution of the Ediacaran-Silurian Nanhua foreland basin, South China. Gondwana Research 28, 1449–1465.
Yu, J.H., O'Reilly, S.Y., Wang, L.J., Griffin, W.L., Zhang, M., Wang, R.C., Jiang, S.Y., Shu, L.S., 2008. Where was South China in the Rodinia supercontinent?: evidence from U-Pb geochronology and Hf isotopes of detrital zircons. Precambrian Research 164, 1–15.
Yu, J.H., O'Reilly, S.Y., Wang, L.J., Griffin, W.L., Zhou, M.F., Zhang, M., Shu, L.S., 2010. Components and episodic growth of Precambrian crust in the Cathaysia Block, South China: evidence from U-Pb ages and Hf isotopes of zircons in Neoproterozoic sediments. Precambrian Research 181, 97–114.
Zhang, S.B., Zheng, Y.F., 2013. Formation and evolution of Precambrian continental lithosphere in South China. Gondwana Research 23, 1241–1260.

Zhao, G.C., 2015. Jiangnan Orogen in South China: developing from divergent double subduction. Gondwana Research 27, 1173–1180.
Zhao, L., Guo, F., Fan, W.M., Li, C.W., Tan, X.F., Li, H.X., 2010. Crustal evolution of the Shiwandashan area in South China: zircon U-Pb-Hf isotopic records from granulite enclaves in Indo-Sinian granites. Chinese Science Bulletin 19, 2028–2038.
Zhao, L., Guo, F., Fan, W., Li, C., Qin, X., Li, H., 2012. Origin of the granulite enclaves in Indosinian peraluminous granites, South China and its implication for crustal anataxis. Lithos 150, 209–226.
Zhao, K.D., Jiang, S.Y., Chen, W.F., Chen, P.R., Ling, H.F., 2013. Zircon U-Pb chronology and elemental and Sr-Nd-Hf isotope geochemistry of two Triassic A-type granites in South China: implications for petrogenesis and Indosinian transtensional tectonism. Lithos 160–161, 292–306.
Zhao, Z.F., Gao, P., Zheng, Y.F., 2015. The source of Mesozoic granitoids in South China: integrated geochemical constraints from the Taoshan batholith in the Nanling Range. Chemical Geology 395, 11–26.
Zhao, K., Xu, X.S., Erdmann, S., 2017a. Crystallization conditions of peraluminous charnockites: constraints from mineral thermometry and thermodynamic modelling. Contributions to Mineralogy and Petrology 172.
Zhao, K., Xu, X.S., Erdmann, S., Liu, L., Xia, Y., 2017b. Rapid migration of a magma source from mid- to deep-crustal levels: insights from restitic granulite enclaves and anatectic granite. Geological Society of America Bulletin 129 (doi: 10.1130 / B31462.1).
Zheng, Y.F., 2012. Metamorphic chemical geodynamics in continental subduction zones. Chemical Geology 328, 5–48.
Zheng, J.H., Guo, C.L., 2012. Geochronology, geochemistry and zircon Hf isotopes of the Wangxianling granitic intrusions in South Hunan Province and its geological significance. Acta Petrologica Sinica 28, 75–90 (in Chinese with English abstract).
Zheng, Y.-F., Chen, Y.-X., 2016. Continental versus oceanic subduction zones. National Science Review 3, 495–519.
Zheng, Y.-F., Chen, R.-X., 2017. Regional metamorphism at extreme conditions: implications for orogeny at convergent plate margins. Journal of Asian Earth Sciences 145, 46–73.
Zheng, Y.-F., Zhao, Z.-F., Wu, Y.-B., Zhang, S.-B., Liu, X., Wu, F.-Y., 2006. Zircon U–Pb age, Hf and O isotope constraints on protolith origin of ultrahigh-pressure eclogite and gneiss in the Dabie orogen. Chemical Geology 231, 135–158.
Zheng, Y.-F., Xia, X.-X., Chen, R.-X., Gao, X.-Y., 2011. Partial melting, fluid supercriticality and element mobility in ultrahigh-pressure metamorphic rocks during continental collision. Earth-Science Reviews 107, 342–374.
Zheng, Y.-F., Xiao, W.J., Zhao, G.C., 2013. Introduction to tectonics of China. Gondwana Research 23, 1189–1206.
Zhou, X.M., Sun, T., Shen, W., Shu, L., Niu, Y., 2006. Petrogenesis of Mesozoic granitoids and volcanic rocks in South China: a response to tectonic evolution. Episodes 29, 26–33.